Identifying Type III Secretion System Effectors and Interacting Proteins in Plant Growth-Promoting *Pseudomonas syringae* GR12-2

by

Emma Lewis

BSc in Biology, University of New Brunswick, 2020

A Thesis Submitted in Partial Fulfillment
of the Requirements for the Degree of

Master of Science

in the Graduate Academic Unit of Biology

Supervisor: Cheryl Patten, PhD, Biology

Examining Board: Timothy Erickson, PhD, Biology
Yang Qu, PhD, Chemistry

This thesis is accepted by the

Dean of Graduate Studies

THE UNIVERSITY OF NEW BRUNSWICK

August, 2023

ABSTRACT

The type III secretion system (T3SS) secretes effector proteins that contribute to the virulence of *Pseudomonas syringae* pathovars. The plant growth-promoting strain *P. syringae* GR12-2 possesses a Rhizobiales-type T3SS of unknown function, although previous research showed that it is not required for plant interactions. This research aimed to determine the function of the *P. syringae* GR12-2 T3SS by identifying secreted effectors. Mass spectrometry identified several alginate biosynthesis proteins and a predicted T3SS chaperone exclusively in the extracellular medium of the wild-type but not T3SS mutant strains. Affinity purification of proteins that interacted with the predicted T3SS chaperone included several that function in cell wall synthesis and remodelling. Confirmation of the candidate effectors' interaction with or secretion by the T3SS will provide insight into potentially novel functions of the T3SS in *P. syringae* GR12-2.

ACKNOWLEDGEMENTS

Foremost, thank you to Dr. Cheryl Patten for giving me the opportunity to study and conduct research at UNB. I am grateful for her support and guidance over the years. Also, I would like to thank Dr. Shawn MacLellan and Dr. Bryan Crawford for agreeing to be members of my supervisory committee and offering their time and assistance. In addition, thank you to the numerous Department of Biology members who have helped me when troubleshooting, lent me their expertise, and offered helpful suggestions.

Table of Contents

List of Tables

List of Figures

Chapter 1: *Pseudomonas syringae* GR12-2, a Plant Growth Promoting Rhizobacterium

Pseudomonas syringae is a gram-negative, rod-shaped bacterium that is a well-known plant pathovar with an extensive host range (Katagiri *et al.*, 2002). Over 50 pathogenic strains of *P. syringae* have been identified, causing the species to be one of the most common plant pathogens infecting economically important crops (Xin *et al.*, 2018). Although it is predominantly considered a plant pathogen, several *P. syringae* plant growth-promoting strains have been identified, such as *P. syringae* 260-02 (Passera *et al.*, 2019) and *P. syringae* GR12-2 (Lifshitz *et al.*,1987; Blakney & Patten, 2011).

P. syringae GR12-2 is a plant growth-promoting rhizobacterium (PGPR) isolated from Canadian Arctic grass roots (Lifshitz *et al.*, 1986) that enhances root development of canola and several other crops (Lifshitz *et al.*,1987; Hall *et al.*, 1996). Based on phenotypic characterization, the bacterium was originally identified as *Pseudomonas putida*; however, molecular analyses revealed that the strain shares 99% nucleotide sequence identity of 16S rRNA genes with the *P. syringae* pathovars (Blakney & Patten, 2011). This result is supported by the analysis of four housekeeping genes, which showed that the GR12-2 strain and *P. syringae* form a monophyletic group distantly related to *P. putida* (Blakney & Patten, 2011).

PGPR, such as *P. syringae* GR12-2, are found in the rhizosphere, which is the zone of soil around plant roots with high levels of microbial activity (Vejan *et al.*, 2016). The PGPR exist in mutualistic relationships with their host plants, providing benefits to the plant in return for sugars, amino acids, vitamins, or other compounds exuded by the plant's roots (Ahemad & Kibret, 2014; Lugtenburg & Kamilova, 2009). Rhizobacterium can promote plant growth through direct or indirect mechanisms. Direct mechanisms can include increasing abiotic stress tolerance, stimulating root growth, and facilitating resource acquisition such as the fixation of nitrogen, solubilization of phosphate or the secretion of siderophores for chelating iron (Glick, 2012; Vejan *et al.*, 2016). Rhizobacterium can also directly benefit host plants by producing phytohormones such as ethylene and auxins (Vejan *et al.,* 2016). Indirect mechanisms include reducing the effect of disease on the host plant through biocontrol of pathogens by secreting antibiotics or enzymes such as chitinase with antifungal properties, inducing systemic resistance against the pathogens, and competing with pathogens for resources (Lugtenburg & Kamilova, 2009; Vejan *et al.*, 2016).

The *P. syringae* GR12-2 genome was sequenced and compared to the genomes of well-studied *P. syringae* pathovars to identify genes that may function in plant growth-promotion (Patten *et al.*, 2016). The genome sequence revealed the presence of a type III secretion system (T3SS) gene cluster in the GR12-2 strain. A T3SS is commonly present and well-studied in *P. syringae* pathovars as it functions to secrete effectors that aid in virulence by suppressing host plant defense responses (Alfano & Collmer, 2004); however, little is known about the role of this system in plant-beneficial bacteria.

The T3SS is a well-conserved protein export pathway often utilized by gram-negative bacteria to secrete effector proteins into a host cell (Figure 1.1; Portaliou *et al.*, 2016). The overall structure of the T3SS resembles a syringe, with the core structure made up of a highly conserved transmembrane injectosome (Portaliou *et al.*, 2016). The injectosome can be divided into three main components; the extracellular segment, the

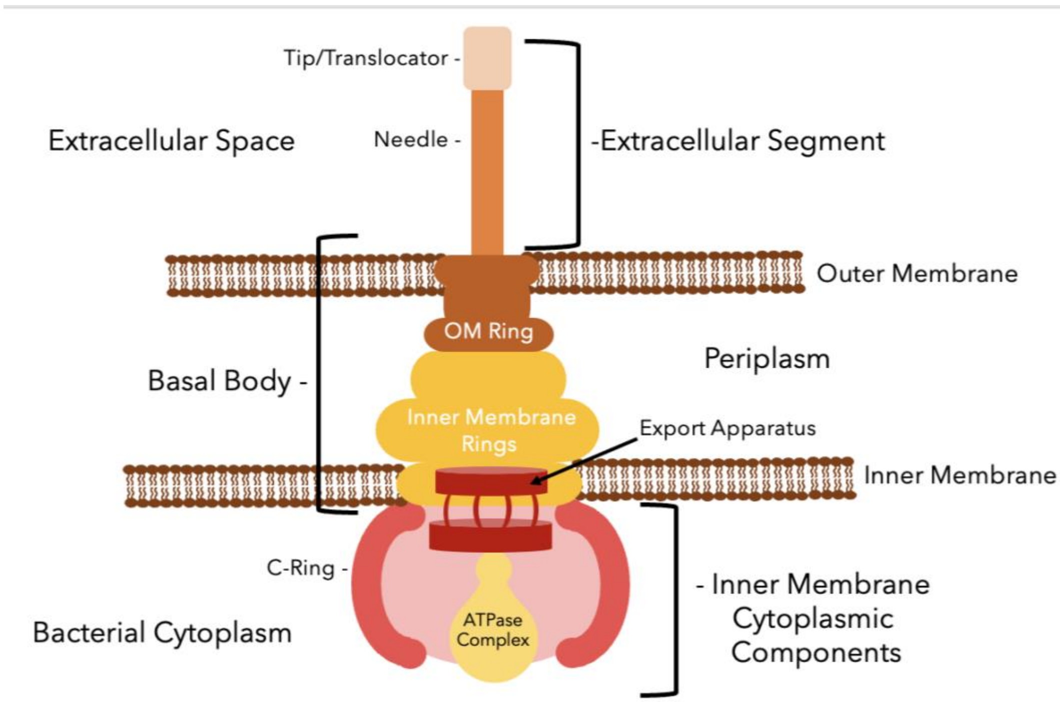

Figure 1.1 General injectosome structure of a type III secretion system in gram negative bacteria (Deng *et al.*, 2017; Portaliou *et al.*, 2016). OM ring, outer membrane ring; C-Ring, cytoplasmic ring.

basal body, and the inner membrane cytoplasmic components. The basal body crosses both membranes of the gram-negative bacteria and is composed of stacked toroidal ring proteins and the export apparatus. Effectors are secreted through the basal body and extracellular needle structure. The extracellular segment includes the needle-like translocon that starts at the outer bacterial membrane and basal body to the tip and translocator pore at the host membrane. The inner cytoplasmic components consist of an ATPase (HrcN) and a cytoplasmic ring, forming the sorting platform. The cytoplasmic ring interacts with the basal body and acts as a vessel for the ATPase. The ATPase is held in place by two accessory components, the stator and the stalk (Portaliou *et al.,* 2016). Effectors secreted by the T3SS are typically targeted to the apparatus in complexes with their cognate chaperones, are disassociated from their chaperones and partially unfolded by the ATPase at the sorting platform, travel through the export apparatus pore formed by HrcV, through the inner rod that lines the basal body rings, through the needle, and finally through the translocator pore into the target host (Deng *et al.,* 2017; Portaliou *et al.,* 2016). The *P. syringae* GR12-2 T3SS gene cluster encodes the essential structural components of the secretion apparatus, with a gene predicted to encode the needle (translocon) HrpK found elsewhere in the genome (Patten *et al.,* 2016).

T3SSs are most commonly studied in phytopathogens, and have a generally ubiquitous function in suppressing host immune responses (Alfano & Collmer, 2004). Effectors secreted by T3SSs in pathogenic *P. syringae* strains have been found to suppress pathogen/microbial-associated molecular pattern (PAMP/MAMP)-triggered immunity (PTI; Macho & Zipfel, 2015), as well as the hypersensitive response of localized cell death (Alfano & Collmer, 2004). While effectors secreted by T3SSs may have roles other than those in plant immune response suppression, the interference in immune response to allow for bacterial colonization is the major function in phytopathogens.

Previous phylogenetic analysis of T3SS genes revealed that *P. syringae* GR12-2 has a *hrp-hrc*3 (hypersensitive response and pathogenicity-hypersensitive response and conserved 3) or Rhizobium conserved (Rhc) T3SS (Cook, 2016), different from *hrp-hrc1* and *hrp-hrc2* T3SSs found in most *P. syringae* pathovars that induce disease or suppress immune responses in plants (Gazi *et al.,* 2012; Tampakaki, 2014). Genome analysis has revealed the presence of a T3SS, from four different T3SS families, in 55 PGPR *Pseudomonas* strains. Three of these were similar to the Rhc T3SS (Zboralski *et al.,* 2022). The Rhc T3SS in plant growth-promoting *Pseudomonas* species may function in biocontrol of other bacteria, fungi, and oomycetes, as well as impairing symbiotic relationships between the host plant and soil fungi, or other currently unknown functions (Biessy *et al.,* 2019; Cusano *et al.,* 2010; Zboralski *et al.,* 2022). Some T3SS effectors in PGPR have been shown to function in suppressing plant immune responses in order to proceed with infection, similar to pathogenic T3SSs (Jiménez-Guerrero *et al.,* 2022; Tampakaki, 2014). A T3SS in PGPR *Bradyrhizobium elkanii* activates nodulation signaling in host plants in the absence of Nod factors, which were assumed to be essential in the nodulation process (Okazaki *et al.,* 2013). However, with so few functions of the T3SSs and secreted effectors validated, the role of T3SSs in plant-beneficial bacteria is not fully elucidated (Jiménez-Guerrero *et al.,* 2022; Tampakaki, 2014; Zboralski *et al.,* 2022).

This project aims to further understand the role of the T3SS in the PGPR *P. syringae* GR12-2. To understand the secretion system's role, this project focused on the identification of effectors secreted by the T3SS and proteins that interact with components of the secretion apparatus, such as T3SS structural proteins HrcV and HrcN, and a predicted T3SS chaperone. HrcN is a predicted ATPase in the T3SS. HrcN oligomerizes into a hexameric ring with an internal pore diameter of 2.5-3 nm. The ATPase interacts with chaperone/effector complexes and functions in the dissociation of the complex and unfolding of the effector proteins for secretion by ATP hydrolysis and proton motive force (Akeda & Galán, 2005; Izoré *et al.*, 2011; Portaliou *et al.*, 2016; Pozidis *et al.*, 2003). HrcV is a predicted inner membrane gate protein that forms a nonameric ring with a 5 nm pore. The gate protein can regulate secretion by changing its cytoplasmic portion's binding affinities for chaperone/effector complexes. Proteins unfolded or partially unfolded from previous ATPase interaction can then pass through the pore for secretion (Abrusci *et al.*, 2012; Portaliou *et al.*, 2016). Thus, HrcN and HrcV are expected to interact with and to be essential for secretion of effector proteins.

Secreted effector proteins are usually targeted to the T3SS apparatus by chaperone proteins (Portaliou et al., 2016). There are several functions of chaperones associated with the T3SS, such as stabilizing effectors in the bacterial cytoplasm, preventing the association of effectors with inappropriate proteins before secretion, or maintaining effectors in an unfolded state for secretion (Alfano & Collmer, 2004; Page & Parsot, 2002). Chaperones have also been observed to regulate secretion in T3SSs, as well as affecting the hierarchy of effector secretion by influencing the concentration of secretion complexes (Alfano & Collmer, 2004; Page & Parsot, 2002; Portaliou *et al.*, 2016). Chaperones for the T3SS function in different stages of secretion, and have been sorted into three main classes based on when they function. There are three stages of secretion: early-stage secretion of substrates that form the T3SS inner rod and needle, middle-stage secretion of substrates that form the translocator pore and needle tip, and late-stage secretion of effector proteins (Deng *et al.,* 2017). Class I chaperones bind effector proteins during late-stage secretion. Class II chaperones typically contain three tetracopeptide repeat (TPR) motifs and form complexes with components of the T3SS during early-stage secretion. Class III chaperones also typically have TPR motifs and target structures like the needle-forming components of the T3SS in the middle stage of secretion (Izoré *et al.,* 2011; Portaliou *et al.,* 2016).

A TPR motif consists of 34 amino acids, often repeated in tandem in many proteins (Bröms *et al.,* 2006; Cerveny *et al.,* 2013). The TPR structure consists of two alpha-helical subdomains antiparallel to each other. When multiple TPRs are present in a protein, the collective subdomains form a superhelical structure, which allows for binding to target proteins via an amphipathic channel (Cerveny *et al.,* 2013). The TPR motif allows for the formation of multiprotein complexes, and proteins with TPR motifs are known to function in virulence (Cerveny *et al.*, 2013), cell cycle control (D'Andrea, 2003), as secretion system regulators (Pallen *et al.*, 2003), and chaperones (Portaliou *et al.,* 2016). T3SS class II and III chaperones with TPR motifs have been found in *Yersinia* (Edqvist *et al.*, 2006), *Shigella* (Cerveny *et al.*, 2013), and *Pseudomonas* species (Bröms *et al.,* 2006; Portaliou *et al.,* 2016). A gene (AFK24_20305) in the *P. syringae* GR12-2 T3SS gene cluster encodes a protein that is predicted to be a chaperone based on the presence three TPR motifs in its sequence (Stocek, 2018). Identification of proteins that interact with the predicted chaperone may provide clues as to the function of the T3SS in this bacterium.

The T3SS in *P. syringae* GR12-2 was initially hypothesized to promote plant colonization by secreting effector proteins into the plant cells that suppress the plant immune response. T3SS effectors are known to suppress PTI through mechanisms such as degrading PAMP/MAMP receptors or interfering in the signaling to induce PTI responses such as the generation of reactive oxygen species and localized deposition of callose (Busciall *et al.*, 2019; Macho & Zipfel, 2015). However, infection of tobacco leaves with mutant *P. syringae* GR12-2 strains with markerless deletions in three key T3SS structural proteins, HrcN, HrcV and HrpK (the translocon), did not elicit a defense response (Jong, unpublished). Also, the ability to promote elongation of roots in inoculated canola seedlings was not significantly different among *P. syringae* GR12-2 wild-type and mutant strains suggesting that root colonization was not impacted by the loss of the T3SS components (Jong, unpublished). These results suggest that the *P. syringae* GR12-2 T3SS has a function other than facilitating plant interactions.

This study attempted to further understand the role of the T3SS in *P. syringae* GR12-2 by identifying effector proteins through two approaches. The first approach aimed to identify the secreted effectors by mass spectrometry. Proteins absent in the extracellular medium of both *hrcV*$^{-}$ and *hrcN*$^{-}$ mutant *P. syringae* GR12-2 strains but present in the wild-type strain were identified as candidate effectors. The second approach aimed to identify effector proteins that interact with components of the secretion apparatus, specifically the HrcN ATPase and the HrcV gate protein, via proximity dependent labeling, and the predicted TPR motif-containing chaperone, by affinity purification of proteins associated with a chaperone carrying a FLAG epitope. These methods identified several proteins of interest whose potential role in type III secretion and plant interactions require further analysis for confirmation of their function, and provide a starting point for further exploration.

Chapter 2: Identification of Secreted Effectors using Mass Spectrometry

Introduction

P. syringae pathovars commonly have a T3SS, as it functions to secrete effectors that aid in virulence by suppressing host plant defense responses (Alfano & Collmer, 2004). Interestingly, the PGPR *P. syringae* GR12-2 has a Rhc *hrp-hrc3* T3SS (Cook, 2016), different from the *hrp-hrc1* and *hrp-hrc2* T3SSs found in *P. syringae* pathovars (Gazi *et al.*, 2012; Tampakaki, 2014), although its function is currently unknown. The objective of this research is to further understand the T3SS's role in *P. syringae* GR12-2 by identifying secreted proteins.

One approach to determine the function of the *P. syringae* GR12-2 T3SS is to identify the secreted effector proteins. For this, mutant strains of *P. syringae* GR12-2 were generated with precise, markerless deletions in two genes encoding proteins of the T3SS apparatus (Patten, unpublished), and proteins secreted by the mutants were compared to those secreted by the wild-type strain. The deletions occur in *hrcN*, encoding a predicted ATPase that partially unfolds effectors prior to secretion, and *hrcV*, encoding a predicted inner membrane gate protein that controls effector export (see Chapter 1). Deletion or alteration of gate protein in *Shigella flexneri* has been shown to abolish or decrease the secretion of the translocator protein IpaB through the T3SS (Abrusci *et al.*, 2012). Studies have also shown evidence suggesting that without the ATPase's chaperone-releasing and protein unfolding abilities, secretion through the T3SS of effectors in *Salmonella enterica* (Akeda & Galán, 2005), and needle-forming components in *Escherichia coli* (EPEC; Chen *et al.*, 2013), can be diminished or halted.

Proteins absent in the extracellular medium of both mutant strains but present in the wild-type strain were identified by liquid chromatography-tandem mass spectrometry (LC/MS/MS). Specifically, the method of bottom-up mass spectrometry (MS), commonly used to analyze a mixture of unidentified proteins, was used for this study (Resing & Ahn, 2004). In this method, mixed proteins are initially broken down into peptide fragments by tryptic digestion. The fragments are then separated via liquid chromatography (LC), and then peptide masses are determined by data-dependent tandem MS/MS. As precursor ions are continuously being eluted via LC, mass spectra are recorded in an initial MS scan, and the mass spectrometer separates a set amount of precursor ions that are either isolated based on predetermined criteria or are those of the highest abundance (Barkovits *et al.,* 2020; Zhang *et al.,* 2013). Each isolated precursor is further fragmented, and another data-dependent MS/MS scan is run for each of the fragmented precursor ions (Glish & Vachet, 2003; Thomas *et al.,* 2022). The mass spectrometer measures the mass-to-charge (*m/z*) ratio for each fragment ion and generates spectra for each ion, which shows the ion abundance and *m/z* values as a plot (Glish & Vachet, 2003). These spectra are then compared to databases of spectra from proteins or peptide fragments that have been "theoretically" digested. Algorithms match the MS spectrum data to a peptide (Wysocki *et al.,* 2005), and the peptides are then assigned to their parent proteins. A peptide can be assigned to multiple proteins or a single protein. This results in protein identifications with varying degrees of confidence, determined by the overall probability that peptides were assigned to proteins correctly, and the level of confidence in each protein identification must be considered when analyzing MS data (Zhang *et al.,* 2013).

Extracellular secretion of proteins of interest identified by the MS results were further tested using the Nano-Glo® HiBiT Extracellular Detection System (Promega, WI, USA). The assay takes advantage of NanoLuc, an engineered luciferase from the deep-sea shrimp *Oplophorus*, that, when combined with the substrate furimazine, results in intense luminescence (Hall *et al.,* 2012). The luciferase is split into two smaller modified subunits, HiBiT (11 amino acids) and LgBiT (17.6 kDa). The subunits derived from NanoLuc underwent mutagenesis, resulting in three amino acid substitutions in the small subunit, and 16 amino acid substitutions in the larger subunit. The two subunits bind with a high affinity (K_D = 700 pm), which restores the activity of the luciferase (Dixon *et al.,* 2015; Promega, 2017). Therefore, extracellular protein secretion can be detected by expressing proteins of interest with the small HiBiT tag and adding the purified LgBiT subunit, which does not enter cells, and furimazine to the culture media. HiBiT-tagged proteins exposed to the extracellular medium bind to LgBiT, which can be detected by measuring luminescence (Promega, 2017). The Nano-Glo® HiBiT system was chosen over other methods to confirm protein secretion because it requires minimal manipulation of the bacterial cultures that could otherwise disrupt cells. Reducing cell lysis helps avoid the inadvertent release of intracellular proteins that would contaminate the extracellular medium and compromise the assay results.

Methods

Extraction of extracellular proteins from *P. syringae* GR12-2 strains

Bacteria were cultured in M9 minimal media (BD #248510) with 0.4% glucose (M9G) to early stationary phase as previous work confirmed expression of *hrcV* and *hrcN* under these conditions (Cook, 2016; Hynes, 2019). M9G minimal agar plates were streaked with strains GR12-2, J246, and J247 from the -80°C culture stock (Table 2.1). Single colonies were inoculated into three ml of M9G medium and incubated for two days at 27°C. One ml of the seed cultures was inoculated into 20 ml of M9G medium, which was incubated at 27°C for two days until the optical density (OD_{600nm}) reached ~1. Cultures were adjusted for equal cell concentrations, as growth rates varied slightly among the different strains, which had been noted in previous work (Hynes, unpublished; Jong, unpublished). Twenty ml of the cultures were centrifuged at 3000 RPM, 4°C, for ten minutes. The supernatant was filtered using 0.2 µM syringe filters to remove remaining cells, and then 15 ml were transferred to a 15 ml Amicon 3 kDa ultra centrifugal filter device (Millipore #UFC9003) and spun at 4000 RPM, 4°C, for two hours to concentrate the proteins in 700 µl. To precipitate the proteins, an equal volume of 10% trichloroacetic acid (TCA) was added to the concentrated proteins and kept on ice for one hour. The proteins were pelleted by centrifugation (13000 RPM for ten minutes), washed in ice-cold 100% acetone, and air-dried. The pellets were resuspended in 100 µl of 0.1 M phosphate buffer, pH 7.4, at 70°C for 30 minutes. The concentration of proteins in the samples was determined using a Bradford Assay (Bradford, 1976). To visualize protein quality,

Table 2.1. *Pseudomonas syringae* GR12-2 derivatives used in this section of the study.

Strain	*P. syringae* background	Plasmid	Gene of Interest (HiBiT-Tagged)	Source
GR12-2	Wild-type	-	-	Lifshitz *et al.*, 1986
J246	*hrcN*$^{-}$	-	-	Jong and Patten, unpublished
J247	*hrcV*$^{-}$	-	-	Jong and Patten, unpublished
J306	GR12-2	p20650	*AlgK*	Patten, this study
J308	J246	p20650	*AlgK*	Patten, this study
J307	J247	p20650	*AlgK*	Patten, this study
J309	GR12-2	p20305	*TPR* chaperone	Patten, this study
J310	J246	p20305	*TPR* chaperone	Patten, this study
J311	J247	p20305	*TPR* chaperone	Patten, this study
J312	GR12-2	p20320	Predicted effector	Patten, this study
J313	J246	p20320	Predicted effector	Patten, this study
J314	J247	p20320	Predicted effector	Patten, this study
J316	GR12-2	pGent	Gentamicin acetyltransferase (*aacC1*)	Patten, this study

three μg of total protein were loaded on a 4-20% TGX polyacrylamide gel (BioRad) and resolved at 200 V for 30 minutes (see Appendix, Figure 2.1). The gel was stained using Biosafe Coomassie Blue (BioRad #1610786). The protein samples were frozen at -80°C until they were sent for MS analysis to SPARC BioCentre Molecular Analysis, The Hospital for Sick Children, Toronto, Canada.

Mass spectrometry of proteins

Proteins sent to SPARC BioCentre (Toronto, ON) underwent sample preparation and tryptic digestion. LC was performed by separating samples on a 75 µm x 50 cm PepMax RSLC EASY-Spray column using the EASY-nLC 1200 nano-LC system (Thermo Fisher Scientific Inc.). The peptides were analyzed via MS using the Thermo Scientific Orbitrap Fusion Lumos Tribrid mass spectrometer (Thermo Fisher Scientific Inc.). The mass spectra were attained via an initial full MS scan followed by data-dependent MS/MS scans.

Mass spectrometry data analysis

The software used to visualize and compile MS data was Scaffold, version 5.0.1 (Proteome Software Inc., Portland, OR). MS/MS data was analyzed by MS-Amanda Proteome Discover (Dorfer *et al.,* 2014) and Sequest (Eng *et al.,* 1994) and run against the uniport_UP000093104_Pseudomonas_syringae_06072021 database (Patten *et al.*, 2016) assuming tryptic digestion. Each software searched the database with the parameters of a 0.60 Da fragment ion mass error tolerance and a parent ion mass error tolerance of 50 PPM. The fixed modification of carbamidomethylation of cysteine, along with variable modifications including oxidation of methionine, acetylation of a peptide's N-terminus, and deamidation of asparagine and glutamine, were set for Sequest and MS-Amanda Proteome Discover.

For proteins to be considered further in this study, they must have met the following stringent criteria: 1) a probability of at least 99.9% that the protein was identified correctly. This is the protein threshold calculated by the Protein Prophet algorithm (Nesvizhskii *et al.,* 2003); 2) a minimum of five unique, correctly identified peptides per protein. A peptide is included and considered correctly identified if it meets a threshold posterior error probability of 95% (peptide threshold) as calculated by Percolator (Käll *et al.,* 2008); 3) a minimum total spectrum count of five. The total spectrum count given for each protein by Scaffold is all the identified spectra associated with a protein, including spectra unique to the protein and those shared with other proteins (Searle, 2010).

Construction of strains to express HiBiT-tagged proteins

To confirm the secretion of proteins of interest identified by MS, the Nano-Glo HiBiT Extracellular Detection System (Promega #N2420) was employed. Genes encoding selected proteins were amplified from *P. syringae* GR12-2 genomic DNA by PCR using primers that included the sequence for the addition of a C-terminal HiBiT affinity tag (11 amino acids) and for restriction enzyme recognition sites to facilitate cloning (Table 2.2). To construct a control for leakage of intracellular proteins, the gene

Table 2.2. Plasmids introduced into *Pseudomonas syringae* GR12-2 and its derivatives in this section of the study.

Plasmid	Description	Source
pHERD26T	Vector backbone, confers tetracycline resistance and contains an arabinose inducible promotor preceding the multiple cloning site	Qiu *et al.,* 2008b
p20650	Fusion of HiBiT tag fused to the C-terminus of *20650* AlgK (encoded by gene 20650) in pHERD26T	Patten, this study
p20305	Fusion of HiBiT tag fused to the C-terminus of TPR (encoded by gene *20305*) in pHERD26T	Patten, this study
p20320	Fusion of HiBiT tag fused to the C-terminus of a predicted effector (encoded by gene *20320*) in pHERD26T	Patten, this study
pGent	Fusion of HiBiT tag fused to the C-terminus of gentamicin acetyltransferase (encoded by *aacC1*) in pHERD26T	Patten, this study

(*aacC1*) encoding gentamicin N-(3)-acetyltransferase, which confers resistance to gentamicin and is not secreted, was similarly amplified from template pJQ200SK (Quandt & Hynes, 1993) using primers containing a C-terminal HiBiT tag (Table 2.2). PCR products were purified using the QIAquick PCR Purification Kit (Qiagen, Hilden, Germany), digested with the restriction enzymes NcoI (NEB #R0193S) and XbaI (NEB #R0145S) at 37°C overnight, and then heat-inactivated at 80°C. The digested HiBiT-tagged genes were ligated with similarly digested pHERD26T vector (Qiu *et al.*, 2008b). The reactions were transformed into chemically competent *Escherichia coli* (*E. coli*) DH5α cells (NEB #C2987I) following the NEB protocol and plated on LB agar (Fisher Scientific # BP1425-500) plates containing 10 µg/ml tetracycline to select for the presence of pHERD26T and X-gal (100 µg/ml) and isopropyl ß-D-1-thiogalactopyranoside (0.5 mM) to confirm amplicon insertion by blue/white selection. White colonies were streak purified before plasmid isolation using the QIAprep Spin Miniprep Kit (Qiagen #27104) and correct plasmid construction was confirmed by sequencing (Robarts Research Institute, London, ON). Plasmids (Table 2.3) were then introduced into *P. syringae* GR12-2, J246, and J247 by electroporation to generate strains J306-J316 (Table 2.1). To generate electrocompetent cells, *P. syringae* GR12-2 was grown in 50 ml of LB broth at 27°C until an OD_{600nm} of ~0.5-0.6 was reached and then poured into ice-cold tubes and incubated on ice for 10 minutes. Cells were pelleted by centrifugation and resuspended in 20 ml ice-cold 10% glycerol, and subsequent washes were completed with five ml and 0.5 ml of 10% glycerol. Two µl of isolated plasmid and 100 µl of electrocompetent cells were added to electroporation cuvettes and

Table 2.3. PCR primers used in this section of the study for gene amplification, fusion protein construction, construct confirmation, and sequencing. Primer sequences are denoted as follows: uppercase represents gene-specific sequences, lower case represents vector-specific sequences, bold letters represent stop codons, italicized letters represent the reverse complement HiBiT tag sequence, and underlined sequences represent restriction enzyme cut sites of NcoI in forward primers and XhaI in reverse primers.

Primer	Sequence 5’ → 3’	Description	Tm (°C)	Source
20650-F	acatacccATGGGTAGCCCACTACGAAC	Forward primer of *20650* with C-terminal HiBiT tag	72.9	Patten, this study
20650HBT-R	gtcgacttctaga**tca***GCTAATCTTCTTGAACAGCCGCCAGCCGCTCAC*TAGGGGTGCGTCCTCGC	Reverse primer of *20650* with C-terminal HiBiT tag	92.7	Patten, this study
20305-F	acatacccatggATGCCCAAGCGTTTTGCCTC	Forward primer of *20305* with C-terminal HiBiT tag	81.5	Patten, this study
20305HBT-R	gtcgacttctaga**tca***GCTAATCTTCTTGAACAGCCGCCAGCCGCTCAC*GTGGGAATCCACCAGAC	Reverse primer of *20305* with C-terminal HiBiT tag	92.2	Patten, this study
20320-F	acatacccatggATGACCGCAAGTCTCGCAGC	Forward primer of *20320* with C-terminal HiBiT tag	81.9	Patten, this study
20320HBT-R	gtcgacttctaga**tca***GCTAATCTTCTTGAACAGCCGCCAGCCGCTCAC*TTGACCTTTCAATAACG	Reverse primer of *20320* with C-terminal HiBiT tag	88.7	Patten, this study
Gent-F	acatacccatggATGTTACGCAGCAGCAACGA	Forward primer of *aacC1* with C-terminal HiBiT tag	79.9	Patten, this study
GentHBT-R	gtcgacttctaga**tca***GCTAATCTTCTTGAACAGCCGCCAGCCGCTCAC*GGTGGCGGTACTTGGGTCGA	Reverse primer of *aacC1* with C-terminal HiBiT tag	93.9	Patten, this study

electroporated at 1.8 kV. Cells were immediately transferred to one ml of LB broth and recovered at 27°C for 60 minutes. Once recovered, cells were plated on LB agar with four μg/ml tetracycline plates and incubated at 27°C.

HiBiT assays to detect extracellular secretion of proteins

M9G broth with four µg/ml tetracycline was inoculated with the *P. syringae* strains carrying the HiBiT-tagged genes in triplicate or quadruplicate, and incubated at 27°C for 24 hours. M9G broth was inoculated with untransformed *P. syringae* GR12-2 as a control. The cultures were then subcultured to an OD_{600nm} of 0.1 in three ml of M9G/tetracycline broth and incubated for 18 h (late log phase) or 26 h (stationary phase) at 27°C. Fifty µl of the cultures were transferred to a 96-well opaque F-bottom plate (Greiner CellStar), followed by 50 µl of HiBiT reagent containing HiBiT Buffer (Promega #N243A), HiBiT Substrate (Promega #N300A) and LgBiT protein (Promega #N401A) as per the manufacturer's instructions. The plate was quickly moved to a shaking platform (80 rpm) for two minutes in the dark and then to a SpectraMax M5 microplate spectrophotometer (Molecular Devices) to incubate in the dark for another two minutes. Luminescence was measured with an integration time of 0.5 seconds and recorded as relative light units (RLU). The cultures OD_{600nm} was also measured to adjust for differences in cell concentration.

A one-way ANOVA was used to assess significant differences (*P* value less than 0.05) in HiBiT-tagged protein secretion among the strains. The categorical value was the three backgrounds in which the HiBiT-tagged protein were expressed, and the continuous variable was the normalized luminescence measurements (RLU/OD). A Tukey-Kramer HSD pairwise comparison test was performed to determine which means were significantly different with an alpha level of 0.05 (Lee & Lee, 2020). Statistics were done using JMP v7 (SAS Institute Inc, Toronto, ON).

Results

MS data analysis (protein threshold, 99.9%; peptide threshold, 95%; minimum of five matching peptides; minimum of five total spectra) identified 1,061 unique proteins in the extracellular medium of the *P. syringae* wild-type and T3SS mutant strains grown in M9G to early stationary phase, 666 of which were found in the media of all strains (Figure 2.2). Of particular interest were proteins potentially secreted by the T3SS, which are the 67 proteins present only in wild-type *P. syringae* GR12-2 media and not in either of the mutant strains J246 and J247 (Table 2.4). However, proteins in the media from the wild-type strain and only one of the mutant strains were also further considered, with 25 proteins found in GR12-2 and J246 but not J247, and 24 proteins found in GR12-2 and J247 but not J246 (Figure 2.3).

Trends and proteins of interest were evident among the proteins present both exclusively in the media from GR12-2 and in GR12-2 and either J246 or J247 (Table 2.4; Figure 2.3). Interesting proteins included the predicted TPR chaperone encoded in the T3SS locus, the sigma factor AlgU, and four alginate biosynthesis and regulatory proteins encoded in a cluster, or potentially in an operon. Trends in the results included several proteins containing TPR motifs or proteins characterized as lipoproteins.

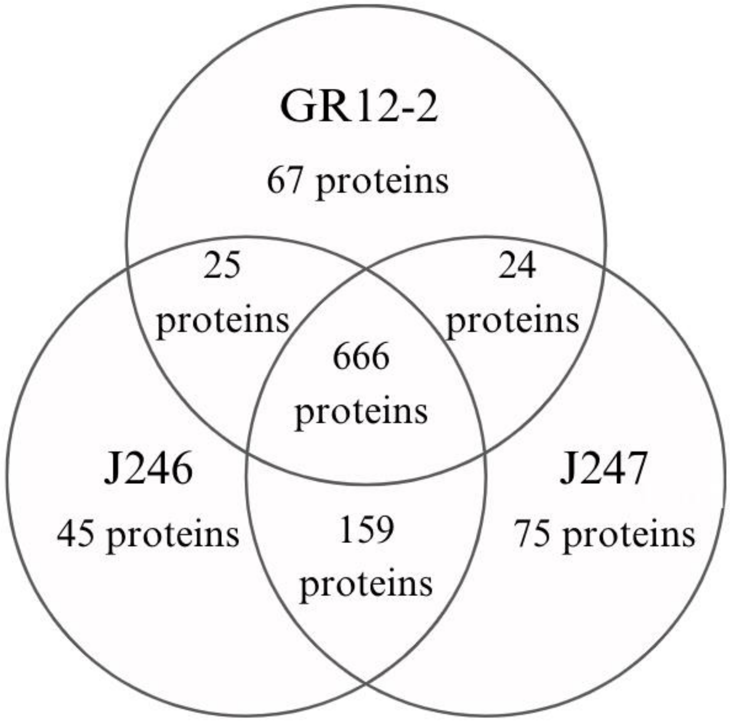

Figure 2.2. A total of 1061 unique proteins were identified via MS in the extracellular medium of *P. syringae* GR12-2, J246, and/or J247. The Venn diagram displays the number of proteins unique to each strain or shared among the strains.

Table 2.4. Proteins identified by MS analysis that were present exclusively in the wild-type *P. syringae* GR12-2.

Identified Protein	Accession Number	Gene*	Total Spectrum Count
Serine/threonine protein kinase	A0A1C7ZAM0	00165	8
Peptidase M42	A0A1C7ZAN0	00225	7
Potassium transporter KefA	A0A1C7ZDA4	00605	9
Integral membrane protein	A0A1C7ZEG3	01110	6
Fimbrial protein	A0A1C7ZCU9	01740	9
Outer membrane lipoprotein Blc	A0A1C7ZCR7	01960	8
Membrane protein	A0A1C7Z9H2	02200	10
Membrane protein	A0A1C7Z9U9	02235	9
Homoserine acetyltransferase	A0A1C7Z9D0	02455	9
Endoribonuclease	A0A1C7ZDH8	02740	5
Alpha-2-macroglobulin	A0A1C7ZBA8	02785	8
Uncharacterized protein	A0A1C7ZDD0	03195	6
ATPase	A0A1C7ZAN2	04495	6
Lipoprotein	A0A1C7ZCG1	04625	10
Endoribonuclease L-PSP	A0A1C7ZBL6	04860	8
Peptide chain release factor RF-3	A0A1C7ZBM6	07415	21
50S ribosomal protein L33	A0A085VIN3	08430	15
Deoxyguanosinetriphosphate triphosphohydrolase	A0A1C7Z8I2	09305	7
Uncharacterized protein	A0A085VLQ6	09430	17
HopJ type III effector protein	A0A1C7Z4K9	10790	6
Peptigoglycan-binding protein LysM	A0A1C7Z6E1	11480	9
YCII domain-containing protein	A0A1C7Z5V3	11530	6
Membrane protein	A0A1C7Z457	11970	6
Transcriptional regulator	A0A1C7Z3A3	14420	11
30S ribosomal protein S18	A0A085V8B3	14600	7
Phosphate-binding protein	A0A1C7Z2U1	15090	9
Transketolase	A0A1C7Z2M6	15205	5
Uncharacterized protein	A0A1C7Z465	15690	5
Beta-glucosidase	A0A1C7Z3H7	16590	12
Lipoprotein	A0A1C7Z3P3	16985	6

LexA repressor	A0A085V4V5	17800	6
Membrane protein	A0A1C7Z6B3	18155	7
Uncharacterized protein	A0A1C7Z440	18165	9
Acetyltransferase	A0A085UQX0	18480	10
Cytochrome C	A0A1C7Z0L0	18550	9
Lipoprotein	A0A1C7Z0U8	18595	8
Catalase	A0A1C7Z0M0	18610	7
DNA-binding protein	A0A1C7Z335	18690	8
Dimethylallyltransferase	A0A1C7Z0H8	18780	7
Uncharacterized protein	A0A1C7Z2S5	19515	6
Peptigoglycan-binding protein LysM	A0A1C7Z2X3	19725	8
Lipoprotein	A0A1C7Z1R0	19850	8
TPR domain-containing protein	A0A1C7Z188	20305	5
Alginate lyase, AlgL	A0A1C7Z3M2	20640	11
Alginate regulatory protein, AlgE	A0A1C7YZM2	20645	19
Alginate biosynthesis protein, AlgK	A0A1C7YZE9	20650	18
Alginate biosynthesis protein, Alg44	A0A1C7Z004	20655	11
GTP-binding protein	A0A1C7Z1F4	21460	8
Pilus assembly protein PilW	A0A1C7YYY4	21480	9
Serine O-acetyltransferase	A0A1C7Z4A1	21535	5
Thiamine pyrophosphate-binding protein	A0A1C7Z1D2	21780	5
Peptidoglycan-binding protein LysM	A0A1C7Z1N4	22065	6
Sugar ABC transporter ATPase	A0A1C7YZW0	22215	9
Cell envelope biogenesis protein AsmA	A0A1C7Z2S8	22580	9
Acyl-homoserine lactone acylase subunit beta	A0A1C7YXW9	22825	5
Leucyl-tRNA synthetase	A0A1C7Z0P6	22955	9
Peptidase inhibitor I42	A0A1C7Z2E5	23240	7
RNA polymerase sigma-H factor AlgU	A0A1C7YYF3	23305	8
4-alpha-glucanotransferase	A0A1C7Z200	24045	6
Glycosyltransferase	A0A1C7YW89	26395	11
Lipoprotein	A0A1C7YW67	26405	33
Triosephosphate isomerase	A0A1C7YZ17	26595	8
Ribosomal RNA large subunit methyltransferase	A0A085UMQ5	26615	5
Outer membrane protein assembly factor BamE	A0A1C7YWD7	26675	9
Uncharacterized protein	A0A1C7YWC2	26735	12
50S ribosomal protein L2	A0A085ULP3	27060	6
2-alkenal reductase	A0A1C7YX61	28075	9

*AFK24 removed from gene locus tag

Figure 2.3. Heat map of 49 proteins identified by MS analysis that are present in the media from wild-type *P. syringae* GR12-2 and one of the T3SS mutants (J246 or J247). The heat map represents the total spectrum counts of the indicated protein in media from each strain. The scale on the right shows the range of color intensities for total spectrum counts from 0 to 47.

HiBiT assays were performed to confirm extracellular secretion of candidate effectors expressed with a C-terminal HiBiT tag in *P. syringae* GR12-2, J246 and J47 backgrounds (strains J306-316; Table 2.1). The MS data indicated that proteins TPR and AlgK were present exclusively in the extracellular medium of *P. syringae* GR12-2 (Table 2.4) and therefore these were selected for further testing in the HiBiT assays. In addition, a predicted effector, encoded by AFK24_20320, was included in the HiBiT assay. While not present in the MS data, the protein is encoded within the T3SS locus and was previously predicted to function as a T3SS effector using the algorithm pEffect (Stocek, 2018).

Secretion of the predicted chaperone TPR was supported by the presence of the TPR protein exclusively in the extracellular media of GR12-2 from MS data. A HiBiT assay revealed a significant difference in the luminescence of the extracellular medium among *P. syringae* strains expressing the TPR-HiBiT fusion after growth in M9G for 18 h ($F(2,6) = 5.4357$, $p<0.045$). Luminescence was higher in the J310 culture, with a *hrcN*$^{-}$ background, compared to the J311 culture, with an *hrcV*$^{-}$ background (Figure 2.4). However, this was not reproduced in a repeat assay at 18 h, nor were there significant differences among the strains after growth in M9G for 26 h. These results suggest that the secretion of the TPR protein is not dependent on the T3SS.

Secretion of the AlgK protein was also supported by the MS data, with AlgK present only in the extracellular media of GR12-2. A HiBiT assay showed a significant difference in the luminescence of the extracellular medium among *P. syringae* strains expressing the AlgK-HiBiT fusion after growth in M9G for 26 h ($F(2,6) = 6.0967$,

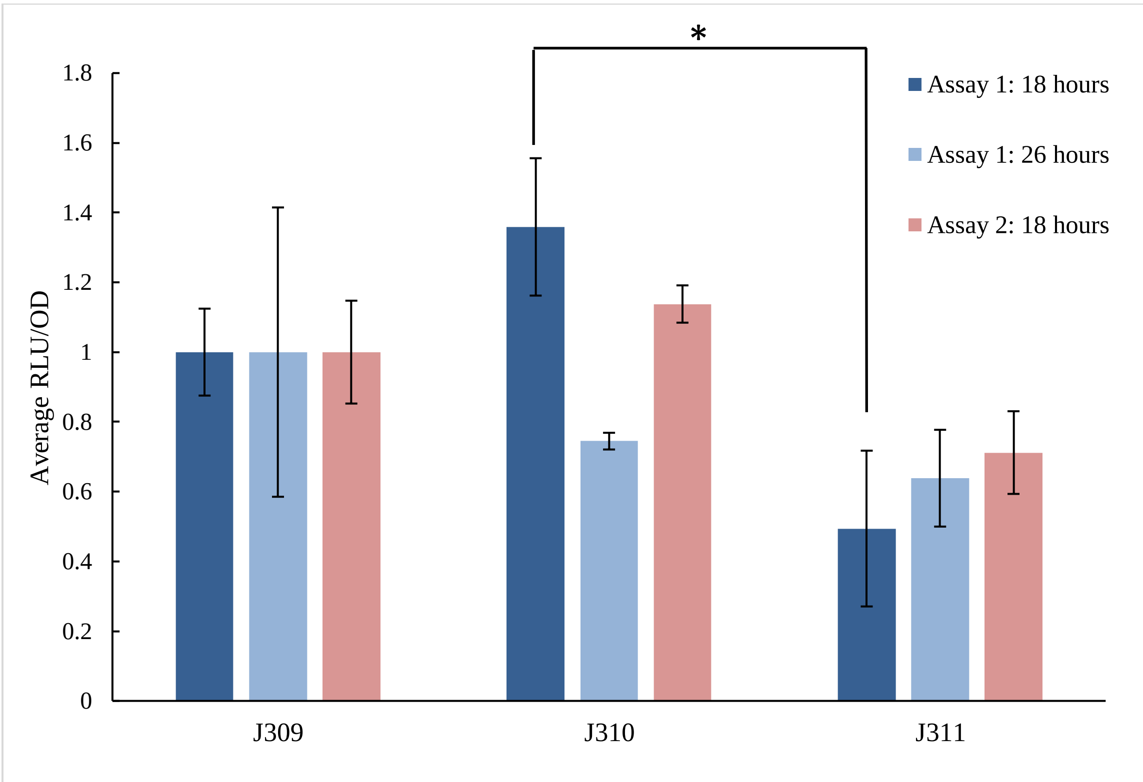

Figure 2.4. Extracellular levels of HiBiT-tagged TPR domain-containing predicted chaperone encoded by gene *20305* in cultures of J309, J310 and J311, with GR12-2, *hrcN*-, and *hrcV*- backgrounds, respectively. Normalized luminescence (RLU/OD) was measured after 18 and 26 hours of growth in M9G using the Nano-Glo® HiBiT Extracellular Detection System. Luminescence values were normalized to those of the J309 strain. Error bars represent standard error of the mean. The asterisk indicates that luminescence was significantly different between the two cultures (Tukey-Kramer HSD, P value <0.05).

p<0.0359). The J307 culture, with an *hrcV*$^{-}$ background, had significantly lower levels of luminescence when compared to the J306 culture, with an wild-type background (Figure 2.5). However, there were no significant differences between the strains after growth in M9G for 18 h. These results suggest that secretion of AlgK may be dependent on the T3SS once the culture passes the late-log phase and into the stationary phase.

Secretion of the protein encoded by AFK24_20320 was predicted, but not supported by the MS data. Secretion was also not supported by the HiBiT assays, as there were no significant differences in luminescence among the cultures of *P. syringae* strains expressing the predicted effector-HiBiT fusion (Figure 2.6). Luminescence values were not higher than those of the J316 control cultures expressing the HiBiT-tagged gentamicin acetyltransferase, which is a cytoplasmic protein that is not secreted extracellularly (Brzezinska *et al.*, 1972). The J316 strain was constructed to detect contamination of the extracellular medium with intracellular proteins from cell lysis. Because LgBiT cannot enter the cell to bind to HiBiT-tagged proteins, luminescence values lower than those seen in the J316 cultures suggests that the predicted effector is not secreted by the wild-type or T3SS mutant strains.

Discussion

MS analysis of extracellular proteins produced by wild-type *P. syringae* GR12-2 and T3SS mutants revealed a large number of secreted proteins. There is no one optimal protocol for determining thresholds such as protein and peptide probability, as each study must weigh the need for increased confidence and smaller data sets, with the potential of

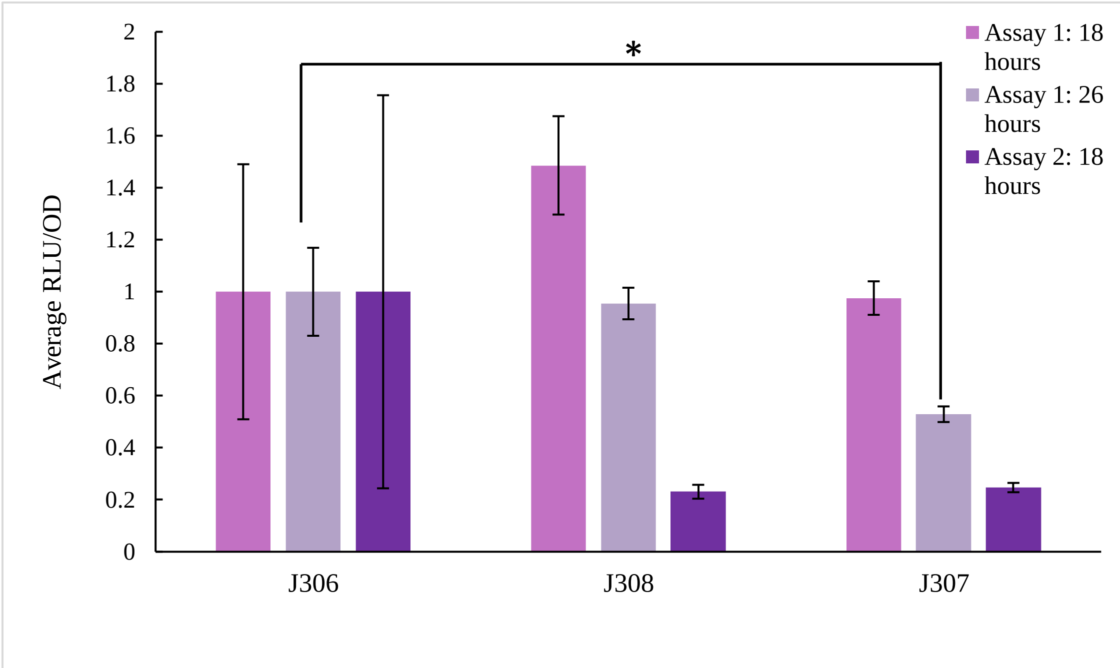

Figure 2.5. Extracellular levels of HiBiT-tagged AlgK encoded by gene *20650* in cultures of J306, J307 and J308 with GR12-2, *hrcV*$^{-}$, and *hrcN*$^{-}$ backgrounds, respectively. Normalized luminescence (RLU/OD) was measured after 18 and 26 hours of growth in M9G using the Nano-Glo® HiBiT Extracellular Detection System. Luminescence values were normalized to those of the J306 strain. Error bars represent standard error of the mean. The asterisk indicates that luminescence was significantly different between the two cultures (Tukey-Kramer HSD, P value <0.05).

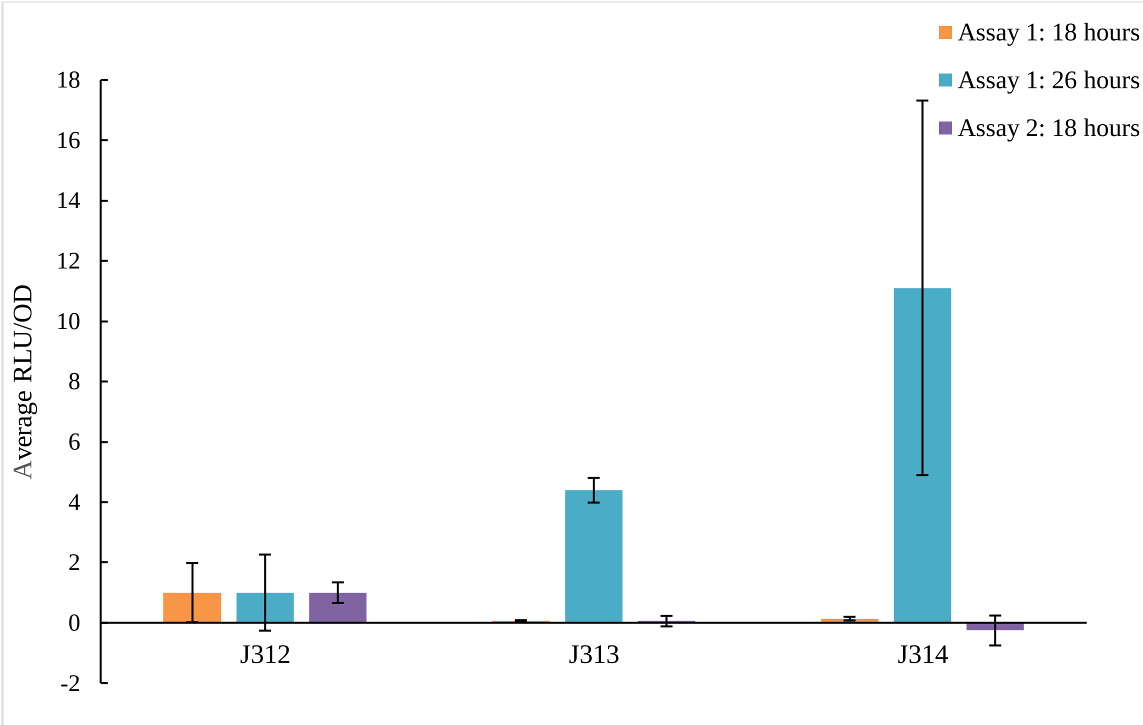

Figure 2.6. Extracellular levels of HiBiT-tagged predicted T3SS effector encoded by gene *20320* in cultures of J312, J313 and J314, with GR12-2, *hrcN*-, and *hrcV*- backgrounds, respectively. Normalized luminescence (RLU/OD) was measured after 18 and 26 hours of growth in M9G using the Nano-Glo® HiBiT Extracellular Detection System. Luminescence values were normalized to those of the J312 wild-type strain. Error bars represent standard error of the mean.

missing relevant results due to stringent restrictions (Baldwin, 2004). In this study, stringent parameters for protein and peptide thresholds, 99.9% and 95%, respectively, and a minimum of five peptides for protein identification using the Scaffold software were employed to increase confidence that the proteins were correctly identified and to assess potential patterns in the dataset (Tabb *et al.*, 2010). As well, due to the semi-stochastic nature of MS analysis, only those proteins with a minimum total spectrum count of five in the wild-type strain were considered. Low-abundance peptides are often missed in LC/MS/MS scans or are not reliably detected, even in replicate MS scans (Barkovits *et al.*, 2020; Tabb *et al.*, 2010). By looking at proteins with higher peptide spectrum counts in the wild-type strain, there is more confidence that their absence in the mutant strains is real rather than due to a lack of detection of low-abundance peptides (Barkovits *et al.*, 2020; Tabb *et al.*, 2010). Application of this stringent criteria resulted in the identification of 67 proteins exclusively present in the extracellular medium of wild-type *P. syringae* GR12-2 and absent in both the *hrcN* mutant J246 and the *hrcV* mutant J247. HrcN and HrcV, a predicted T3SS-specific ATPase and an inner membrane gate protein, respectively, are crucial for the secretion of proteins through the T3SS in other bacteria (Abrusci *et al.*, 2012; Akeda & Galán, 2005; Chen *et al.*, 2013), and therefore the deletion of the encoding genes was expected to generally abolish effector secretion in both mutant strains. However, the biochemical functions of these proteins was determined for the T3SSs found in animal and plant pathogens and their specificities and/or activities may be different for homologous proteins in the *hrp-hrc3* T3SS found in *P. syringae* GR12-2 (Abrusci *et al.*, 2012; Akeda & Galán, 2005; Chen *et al.*, 2013).

Therefore, proteins present in the wild-type strain but missing from one mutant and not the other may be of interest.

Fourteen of the proteins that met the above criteria were characterized as lipoproteins through Scaffold and the *Pseudomonas* Genome Database (Winsor *et al.*, 2015), using the databases Pfam (Mistry *et al.*, 2021), Gene3D (Lewis *et al.*, 2017) and PANTHER (Thomas *et al.*, 2021) (Table 2.4; Figure 2.3). Lipoproteins typically contain a four amino acid motif at the C-terminal end called the lipobox (Wilson & Bernstein, 2016; Zückert, 2014). They are usually secreted to a cell membrane, either to the inner membrane where they are exposed to the periplasm of a gram-negative bacterium, or to the inner leaflet of the outer membrane from which they may be transported to the cell surface or secreted to the extracellular medium (Wilson & Bernstein, 2016). Several of the identified proteins are members of the OmpA family of outer membrane lipoproteins that contain a highly conserved peptidoglycan-binding anchor domain at their C-terminus (Paulsson *et al.*, 2021; Remans *et al.*, 2010). Proteins with an OmpA family domain often function as porins (Chevalier *et al.*, 2017; Freudl *et al.*, 1990; Smith *et al.*, 2007) or as proteins anchored to the outer membrane by a lipid tail (Bouveret *et al.*, 1999). *P. syringae* GR12-2 extracellular, potentially T3SS-dependent, proteins that contain the OmpA family domain are encoded by AFK24_02235 and AFK24_18155, as well as AFK24_26675 (BamE) and AFK24_14420, which are bacterial outer membrane lipoproteins of the OmlA family, the OmlA domain often adjacent to the OmpA domain (Ochsner *et al.*, 1999). The increasing recognition of cell-surface exposed lipoproteins in bacteria (Wilson & Bernstein, 2016) has led to the identification of lipoprotein transport pathways other than the well-studied general secretory (Sec) and localization of lipoproteins (Lol) pathways. Type II and V secretion systems have been observed as alternate modes of lipoprotein outer membrane localization (Konovalova & Silhavy, 2015; Remans *et al.,* 2010; Zückert, 2014). This suggests that alternative methods of lipoprotein transport are plausible and that lipoproteins identified in this study may function as effector proteins secreted by the T3SS.

Several proteins involved in alginate biosynthesis were identified by MS in the medium of wild-type *P. syringae* GR12-2 and not the T3SS mutant strains. In many pseudomonads, alginate is the major exopolysaccharide of the biofilm matrix (Govan *et al.*, 1981; Maunders & Welch, 2017). Biofilms increase the epiphytic survival of bacteria by aiding in plant adhesion and desiccation tolerance (Krishna *et al.,* 2021). Extracellular alginate biosynthesis proteins secreted only by the wild-type strain include AlgL, an alginate lyase encoded by AFK24_20640, AlgF, an alginate regulatory protein encoded by AFK24_20645, AlgK, an alginate biosynthesis protein encoded by AFK24_20650, Alg44, an alginate biosynthesis protein encoded by AFK24_20655 and the sigma factor AlgU encoded by AFK24_23305. The T3SS-dependent secretion of AlgK in stationary phase was supported by significantly higher levels of luminescence in the wild-type strain compared to that of the *hrcV* mutant strain in one of the HiBiT assays. Clusters of genes encoding alginate biosynthesis proteins are present in *Pseudomonas* strains, including *P. syringae* GR12-2, and are predicted to function as a 12-gene operon controlled by the upstream *algD* promotor (Chitnis & Ohman, 1993; Fakhr *et al.,* 1999; Heredia-Ponce *et al.,* 2020; Peñaloza-Vázquez *et al.,* 1997). Alginate biosynthesis occurs in four stages, starting with precursor synthesis in the cytosol, polymerization of precursors in the inner membrane, modification and translocation of alginate chains across the periplasm, and export of mature alginate across the outer membrane (Hay *et al.*, 2013). The Alg protein Alg44 functions in the inner membrane (Boyd & Chakrabarty, 1995; Remminghorst & Rehm, 2006), AlgL (Boyd & Chakrabarty, 1995; Schiller *et al.*, 1993) and AlgF (Boyd & Chakrabarty, 1995; Franklin & Ohman, 1993) function in the periplasm, and AlgK functions in the outer membrane (Boyd & Chakrabarty, 1995; Keiski *et al.*, 2010). The T3SS-dependent secretion of the Alg proteins identified by MS suggests that the secretion system may directly secrete the proteins or have a more secondary effect, such as indirectly regulating Alg protein secretion though the absence of T3SS proteins in the mutants.

Both alginate and the T3SS function in virulence in *Pseudomonas* pathogens (Yu *et al.*, 1999) and the most significant link between the mechanisms is their regulation by the AlgU sigma factor (Schreiber & Desveaux, 2011; Wu *et al.*, 2004). AlgU regulates virulence, flagellin repression, and over-production of alginate, with its regulon comprised of over 800 genes in some *Pseudomonas* strains (Wang, H *et al.*, 2021). MucA is the anti-sigma factor that represses AlgU and is degraded in response to environmental factors, allowing AlgU to regulate genes functioning in plant colonization and epiphytic fitness, osmotic and oxidative stress responses, and down-regulation of flagellin, which reduces PAMP triggered immunity during plant colonization (Bao *et al.*, 2020; Wang, H *et al.*, 2021). AlgU also positively or negatively regulates T3SS expression, sometimes in response to environmental factors, in *P. syringae* pv. *maculicola* ES4326 (Schreiber & Desveaux, 2011), *Pseudomonas aeruginosa* (*P. aeruginosa*; Wu *et al.*, 2004), and *P. syringae* pv. tomato DC3000 (Markel *et al.*, 2016). The shared regulation by AlgU of alginate production and T3SS expression indicates a strong link between the two activities. There is also the possibility of a negative feedback response, where an abolished T3SS in the J246 and J247 strains led to lower levels of AlgU, and consequently lower levels of alginate biosynthesis proteins. As well, with AlgU activation or repression triggered in response to environmental factors such as stress and host immune response, and its expression linked to T3SS expression (Markel *et al.*, 2016; Schreiber & Desveaux, 2011), further research could reveal that the T3SS also responds to environmental stressors. What specific factors trigger T3SS expression could reveal potential functions of the system in PGPR in survival and plant association.

Several proteins of interest in the MS dataset contain TPR domains identified using the Conserved Domain Database (Marchler-Bauer *et al.*, 2016) and Pfam (Mistry *et al.*, 2021), Gene3D (Lewis *et al.*, 2017), and PANTHER (Thomas *et al.*, 2021) in the *Pseudomonas* database (Winsor *et al.*, 2015). TPR domain-containing proteins often mediate protein-protein interactions and function more specifically as chaperones (Cerveny *et al.*, 2013). Class II and III chaperones that interact with translocators and other T3SS structural proteins during the early and middle phases of T3SS assembly contain three TPR motifs (Bröms *et al.*, 2006; Cerveny *et al.*, 2013; Portaliou *et al.*, 2016). Identified proteins in the MS results with a TPR domain associated with chaperone function are the predicted T3SS chaperone TPR, encoded by AFK24_20305, AlgK, encoded by AFK24_20650 (Keiski *et al.*, 2010), PilW, a pilus assembly protein encoded by AFK24_21480 (Koo *et al.*, 2008), and four other proteins encoded by AFK24_26405, AFK24_21460, AFK24_18595, and AFK24_11970 which are of unknown function or a function unrelated to chaperoning. Although TPR appears to be secreted to the extracellular medium and was identified by MS as T3SS-dependent, the results of the HiBiT assay suggest that HrcN and HrcV are not required for its secretion.

The inconsistencies between the MS and Nano-Glo HiBiT analyses may be due to the highly variable luminescence values among some of the replicate cultures in the HiBiT assays. A secondary method should be performed to verify extracellular secretion of candidate effector proteins identified by MS. A potential second method to confirm secretion could be expressing the protein of interest with a FLAG epitope tag. Secretion of the FLAG-tagged fusion protein can be detected in the cell-free culture supernatant by Western blot using an anti-FLAG antibody (Brizzard & Chubet, 1997).

Another factor contributing to the lack of corroboration between the MS and HiBiT assays could be the lack of replicate LC/MS/MS runs. Reproducible results would increase confidence that the identified proteins are T3SS-dependent. Low abundance peptides are not reliably detected by MS (Barkovits *et al.,* 2020; Tabb *et al.,* 2010) and therefore lack of detection of a low abundance protein in the culture medium of J246 and J247 may be lead to the erroneous conclusion that it is absent.

In conclusion, the MS analysis of extracellular proteins of *P. syringae* GR12-2 wild-type and T3SS structural mutants yielded many differentially secreted proteins. However, specific proteins secreted exclusively from GR12-2, indicating secretion by the T3SS, remain to be confirmed using targeted approaches. Additional interesting proteins to be explored are the lipoprotein encoded by AFK24_26405, which has a relatively high total spectrum count, and a protein annotated as a HopJ type III effector; both were found exclusively in the wild-type culture medium.

Chapter 3: Identification of Effectors that Interact with T3SS Proteins Using Proximity- Dependent Labeling

Introduction

Effectors secreted by the T3SS interact with structural components of the injectosome as they are being secreted. Secreted proteins are typically targeted to the T3SS by chaperones in a chaperone-effector complex (Alfano & Collmer, 2004; Portaliou *et al.,* 2016). Chaperone-effector complexes interact with an ATPase (HrcN) located on the cytoplasmic face of the secretion apparatus, which dissociates the complex and unfolds effectors using ATP hydrolysis in preparation for secretion (Akeda & Galán, 2005; Izoré *et al.,* 2011; Portaliou *et al.,* 2016). Effectors then pass through the inner membrane gate protein (HrcV), which forms a pore that unfolded or partially unfolded effectors pass through during secretion (Abrusci *et al*., 2012; Portaliou *et al.,* 2016). This study exploits the interactions among the T3SS structural components, chaperones, and effectors to identify the secreted proteins using proximity dependent labeling.

Proximity-dependent labeling identifies protein-protein interactions using a protein of interest fused to an enzyme that generates a reactive species that tags interacting or neighboring proteins. One of the main advantages of using proximity-dependent labeling is the ability to detect transient interactions and proteins within a one to ten nm radius, depending on the enzyme used (Qin *et al.,* 2021). One method of proximity-dependent labeling is BioID, a protein labeling system that employs the biotin ligase BirA to catalyze the covalent addition of biotin to target proteins. Choi-Rhee *et al*. (2008) used BirA from *E. coli*, which endogenously biotinylates a single protein, the biotin carboxyl carrier protein subunit of the acetyl-CoA carboxylase (Fall *et al.*, 1975). They introduced mutations in the otherwise highly specific BirA to biotinylate proteins more promiscuously. An arginine to glycine substitution in BirA, located within a disordered loop that becomes ordered upon biotin entering the active site self-biotinylates and promiscuously biotinylates other nearby proteins (Choi-Rhee *et al*., 2008). By linking the mutated BirA to a target (bait) protein, any proteins that interact with the BirA fusion protein or are within a ~10 nm distance would be biotinylated (Choi-Rhee *et al*., 2008; Roux *et al*., 2012; Kim *et al.*, 2014). Protein biotinylation can be visualized by Western blotting with streptavidin-AP. Streptavidin binds tightly and specifically to biotin, making it especially suited for detecting biotinylated proteins. Biotinylated proteins can be captured with magnetic streptavidin-linked beads for identification by MS (Roux *et al.* 2012).

This research aims to employ the BioID system to identify effector proteins that interact with the T3SS in *P. syringae* GR12-2. Three bait proteins were expressed as BirA fusion proteins: the predicted TPR-containing chaperone, HrcN, and HrcV of the secretion apparatus. Previously, the BioID system was adapted for use in *Pseudomonas* (MacLellan, unpublished). Plasmids were created to express the BirA^{R55G}-T3SS fusion proteins from an arabinose-inducible promoter in the pHERD26T vector (Jong & MacLellan, unpublished; Qiu *et al.*, 2008b). The BirA protein from *Sinorhizobium meliloti*, modified to contain an arginine to glycine substitution (BirA^{R55G}), was employed due to its smaller size (27 kDa) compared to *E. coli* BirA (35 kDa) and a GC content more similar to that of *Pseudomonas* (MacLellan, unpublished). Other studies have shown that a smaller BirA protein displays successful promiscuous biotinylation (Branon *et al.,* 2018; Kim *et al.,* 2016; Zhao *et al.,* 2021). Plasmids were created containing the *S. meliloti birA*^{R55G} with a sequence encoding a FLAG epitope tag that will be linked at the C- or N-termini of the bait protein. To reduce the potential for BirA^{R55G} to impair the function of the fusion partner and to increase the labeling radius, a flexible poly-glycine linker was included between *birA*^{R55G} and the fusion partner (Varnaitė & Macneill, 2016; Kim *et al.,* 2016); glycine is not expected to interfere with protein function as it is a small, inert amino acid (Pérez-Torres *et al.,* 2016). Expression of the BirA^{R55G}-T3SS fusion proteins in *P. syringae* GR12-2 is expected to biotinylate secreted effectors, which can be identified by MS following affinity purification using streptavidin-linked magnetic beads.

Methods

Construction of *P. syringae* strains that express BirA^{R55G}-T3SS fusion proteins

Previously, plasmids were constructed with *hrcV, hrcN*, or *TPR* inserted in-frame with *birA*^{R55G} such that the fusion protein was expressed with BirA^{R55G} at either the C- or N-terminal end of the T3SS proteins and then transformed into *P. syringae* GR12-2 (Jong, 2018; Table 3.1; Figure 3.1. A control plasmid (pSRM43) containing *birA*^{R55G} and FLAG coding sequences but without a T3SS gene was also constructed. Correct construction of the plasmids was confirmed by sequencing the plasmids (Robarts Research Institute, London, ON). Successful insertion of the T3SS in the correct reading

Table 3.1. *Pseudomonas syringae* GR12-2 derivatives used in this section of the study.

Strain	*P. syringae* background	Plasmid	Gene of Interest	Source
GR12-2	Wild-type	-	-	Lifshitz *et al.*, 1986
J251	GR12-2	pEJCN	*hrcN*	Jong, unpublished
J252	GR12-2	pEJCV	*hrcV*	Jong, unpublished
J253	GR12-2	pEJCT	*TPR* chaperone	Jong, unpublished
J254	GR12-2	pEJNN	*hrcN*	Jong, unpublished
J255	GR12-2	pEJNV	*hrcV*	Jong, unpublished
J256	GR12-2	pELNT	*TPR* chaperone	This study
J257	GR12-2	pSRM43	$birA^{R55G}$	Jong, unpublished
J258	GR12-2	pHERD26T	-	Jong, unpublished

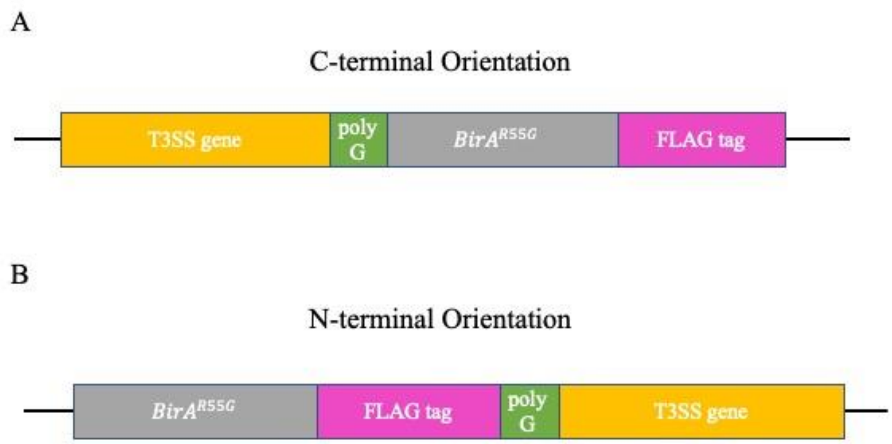

Figure 3.1 Orientation of *birA*^{R55G}-*T3SS* gene fusion constructs. A) Orientation of coding sequences for expression of BirA^{R55G} and a FLAG epitope tag on the C-terminal end of a T3SS protein, linked by a poly-G linker, in pSRM41. B) Orientation of coding sequences for expression of BirA^{R55G} and a FLAG epitope tag on the N-terminal end of a T3SS protein, linked by a poly-G linker, in pSRM42.

frame was confirmed for pEJCN, pEJCV, pEJCT, and pEJNN plasmids but not pEJNV and pEJNT (Jong, unpublished; Table 3.2). The latter two plasmids were therefore reconstructed as follows.

Plasmid backbone pSRM42 was double-digested using XbaI and KpnI-HF (NEB #R3142S) restriction enzymes following the protocol suggested by NEBcloner (Figure 3.2). The digested plasmids were purified using the QIAquick PCR Purification Kit (Qiagen). The *TPR* and *hrcV* genes were PCR amplified from *P. syringae* GR12-2 genomic DNA using NT_F and NT_R and NV_F and NV_R primers, respectively (Table 3.3), and Phusion High-Fidelity DNA Polymerase (NEB # M0530S) following the manufacturer's protocol (Figure 3.2). The PCR products were purified using the QIAquick PCR Purification Kit and then inserted into digested pSRM42 by Gibson assembly at 50°C for one hour. The assembled plasmids were transformed into chemically competent *E. coli* DH5α cells following the NEB protocol. Transformed cells were spread on LB agar with 10 μg/ml tetracycline and incubated at 37°C. Several colonies from each assembly were streak purified and then plasmids were isolated using the QIAprep Spin Miniprep Kit, and PCR was performed to confirm that the Gibson assembly was successful (Figure 3.3).

To prepare electrocompetent cells, *P. syringae* GR12-2 was grown in 50 ml of LB broth at 27°C until an OD_{600nm} of ~0.5-0.6 was reached and then poured into ice-cold tubes and incubated on ice for 10 minutes. Cells were pelleted by centrifugation and resuspended in 20 ml ice-cold 10% glycerol, and subsequent washes were completed with five ml and 0.5 ml of 10% glycerol. Two μl of isolated plasmid and 100 μl of

Table 3.2. Plasmids introduced into *Pseudomonas syringae* GR12-2 and its derivatives in this section of the study.

Plasmid	Description	Source
pHERD26T	Vector backbone, confers tetracycline resistance and contains an arabinose inducible promotor preceding the multiple cloning site	Qiu *et al.,* 2008b
pSRM41	*birA*^{R55G} and FLAG tag in pHERD26T with polyG linker preceding b*irA*^{R55G}	MacLellan, unpublished
pSRM42	*birA*^{R55G} and FLAG tag in pHERD26T with polyG linker following the FLAG tag	MacLellan, unpublished
pSRM43	*birA*^{R55G} and FLAG tag in pHERD26T	MacLellan, unpublished
pEJCN	*birA*^{R55G} and FLAG tag fused to C-terminus of *hrcN* in pSRM41	Jong, unpublished
pEJCV	*birA*^{R55G} and FLAG tag fused to C-terminus of *hrcV* in pSRM41	Jong, unpublished
pEJCT	*birA*^{R55G} and FLAG tag fused to C-terminus of *TPR* in pSRM41	Jong, unpublished
pEJNN	*birA*^{R55G} and FLAG tag fused to N-terminus of *hrcN* in pSRM42	Jong, unpublished
pEJNV	*birA*^{R55G} and FLAG tag fused to N-terminus of *hrcV* in pSRM42	Jong, unpublished
pEJNT	*birA*^{R55G} and FLAG tag fused to N-terminus of *TPR* in pSRM42	Jong, unpublished
pELNV	*birA*^{R55G} and FLAG tag fused to N-terminus of *hrcV* in pSRM42	This study
pELNT	*birA*^{R55G} and FLAG tag fused to N-terminus of *TPR* in pSRM42	This study

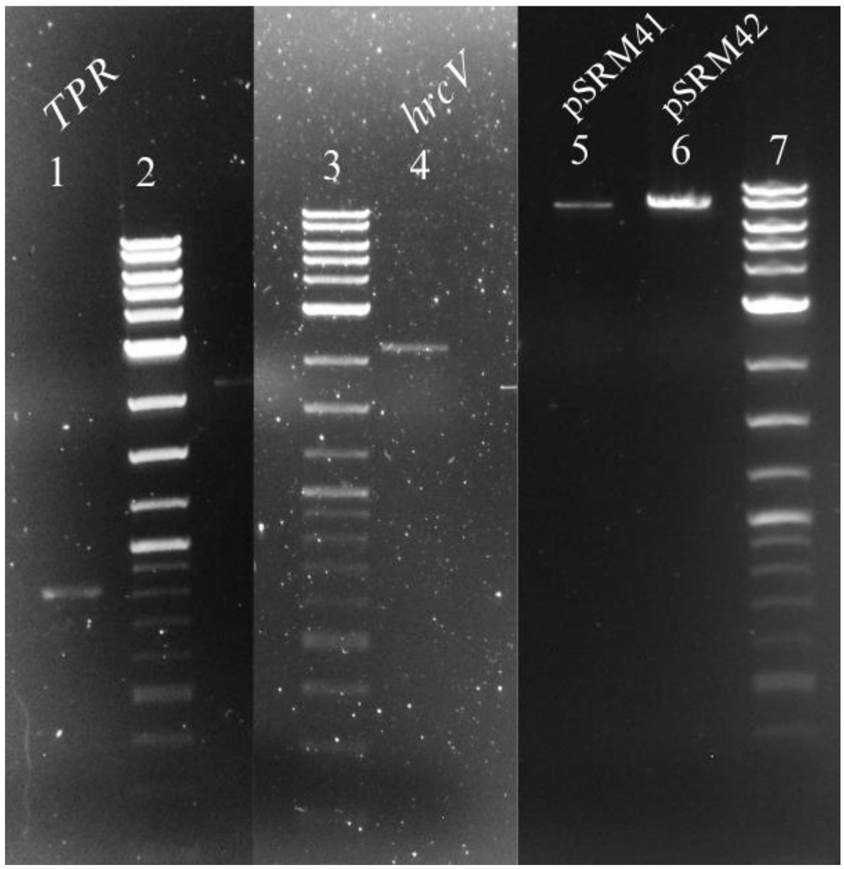

Figure 3.2. PCR products of the *TPR* gene (789 bp, lane 1), and the *hrcV* gene (2139 bp, lane 4) amplified from *P. syringae* GR12-2. Double-digested (XbaI and EcoRI-HF) pSRM41 (lane 5) and double-digested (XbaI and KpnI-HF) pSRM42 (lane 6). A 2-log DNA ladder (NEB #N2300L) was loaded as a size marker (lanes 2, 3, 7).

Table 3.3. PCR primers used in this section of the study for gene amplification, fusion protein construction, construct confirmation, and sequencing. Primer sequences are denoted as follows: uppercase represents gene-specific sequences, and lower case represents vector-specific sequences.

Primer	Sequence 5' → 3'	Description	Tm (°C)	Source
Int_pSRM41	gcactcgctgttggtcg	Forward primer for 3' end of gene of interest in pSRM41	64.7	Jong, unpublished
Int_pSRM42	cggcttctactcgacacg	Forward primer for 5' end of gene of interest in pSRM42	62.3	Jong, unpublished
Pr444	atcgcaactctctactgtttct	Forward primer for pHERD26T vector backbone	58.7	MacLellan, unpublished
Pr445	tgcaaggcgattaagttgggt	Reverse primer for pHERD26T vector backbone	67.5	MacLellan, unpublished
CN_F	ccatgggatctgataagAACATCGTCCTTGAAGACGTCATG	Forward primer for *hrcN* in pSRM41	81.6	Jong, unpublished
CN_R	cataccaccaccacctccTGCCAGCACCTTGCGCAT	Reverse primer for *hrcN* in pSRM41	87.5	Jong, unpublished
CV_F	ccatgggatctgataagATGGTCATGAACAAGCTCAACG	Forward primer for *hrcV* in pSRM41	81.0	Jong, unpublished
CV_R	cataccaccaccacctccTGAGGCATTCGCCATGGAG	Reverse primer for *hrcV* in pSRM41	86.3	Jong, unpublished
CT_F	ccatgggatctgataagCCCAAGCGTTTTGCCTCC	Forward primer for *TPR* in pSRM41	83.0	Jong, unpublished
CT_R	cataccaccaccacctccGTGGGAATCCACCAGACC	Reverse primer for *TPR* in pSRM41	85.6	Jong, unpublished
NN_F	gggtggtggtggtggtaccAACATCGTCCTTGAAGACGTCATG	Forward primer for *hrcN* in pSRM42	87.4	Jong, unpublished
NN_R	gcctgcaggtcgactTCATGCCAGCACCTTGCG	Reverse primer for *hrcN* in pSRM42	87.2	Jong, unpublished

NV_F	gggtggtggtggtggtaccATGGTCATGAACAAGCTCAACG	Forward primer for *hrcV* in pSRM42	87.0	Jong, unpublished
NV_R	gcctgcaggtcgactTCATGAGGCATTCGCCATG	Reverse primer for *hrcV* in pSRM42	86.1	Jong, unpublished
NT_F	gggtggtggtggtggtaccCCCAAGCGTTTTGCCTCC	Forward primer for *TPR* in pSRM42	88.4	Jong, unpublished
NT_R	gcctgcaggtcgactTCAGTGGGAATCCACCAGAC	Reverse primer for *TPR* in pSRM42	84.3	Jong, unpublished

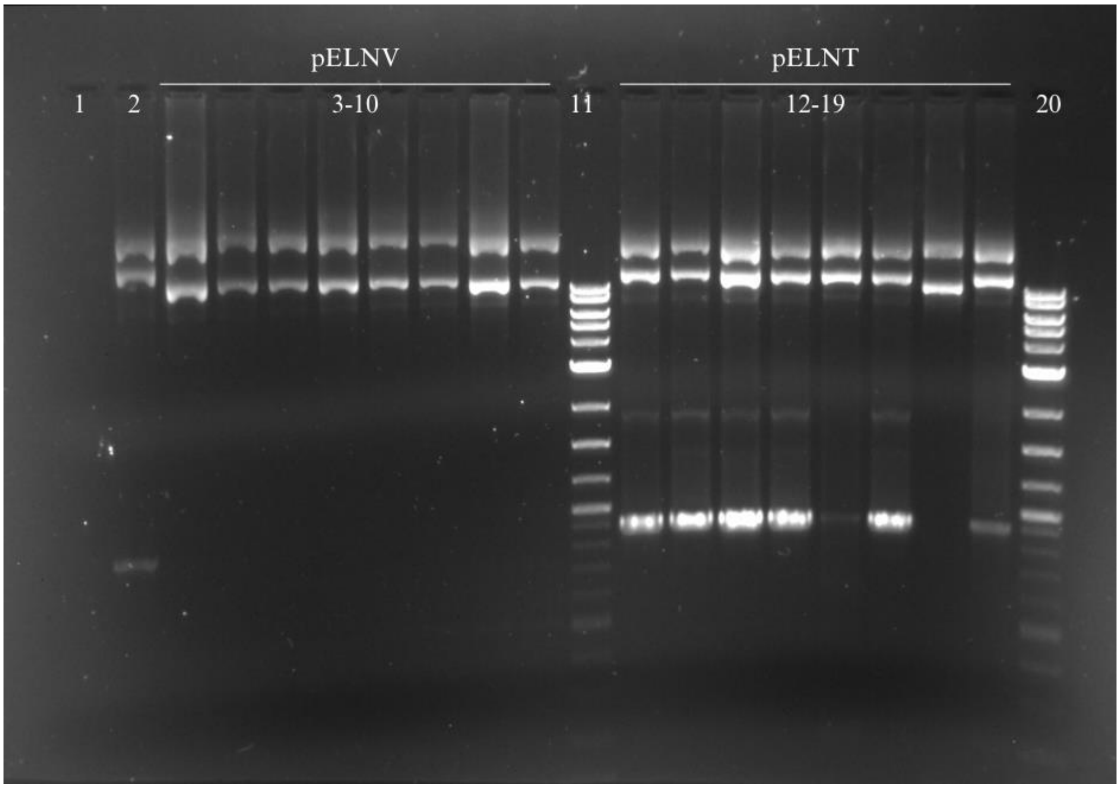

Figure 3.3. Colony PCR to confirm pELNV transformants (lanes 3-10, expected 2,209-bp bands not apparent) and pELNT transformants (lanes 12-19, showing expected 859-bp bands), with a negative control for pELNV colony PCR (lane 1), a pEJNT positive control (lane 2) and 2-log DNA ladder as a marker (lanes 11 and 20).

electrocompetent cells were added to electroporation cuvettes and electroporated at 1.8 kV. Cells were immediately transferred to one ml of LB broth and recovered at 27°C for 60 minutes. Once recovered, cells were plated on LB agar with four μg/ml tetracycline plates and incubated at 27°C. Several colonies were streak purified, grown up in three ml LB broth with four μg/ml tetracycline, and their plasmids were isolated using QIAprep Spin Miniprep Kit (Qiagen). PCR was performed on the isolated plasmids to confirm transformation using two sets of primers: gene-specific forward primer and plasmid-specific pr445 and plasmid-specific primers int_pSRM42 and pr445 (Table 3.3) . Plasmids were also sent for sequencing (Robarts Research Institute, London, ON). An isolated pELNT plasmid yielded the expected bands following PCR with both sets of primers (Figure 3.4) and confirmation from sequencing results indicated that *P. syringae* J256 (Table 3.1) carried the correct plasmid. Insertion of *hrcV* into pSRM42 to generate pELNV was unsuccessful, and the plasmid could not be transformed in *P. syringae* GR12-2.

Anti-FLAG Western blot to assess fusion protein expression

P. syringae strains carrying plasmids with the C-terminal and N-terminal *birA*^{R55G}*-T3SS* fusions and pSRM43 were inoculated in three ml of LB broth with four μg/ml tetracycline in duplicate and grown overnight at 27°C. The overnight seed cultures were subcultured in three ml of the same medium to an OD_{600nm} of ~ 0.1. When growth reached the mid-log phase (OD_{600nm} ~ 0.4-0.6), 20% L-arabinose was added to a final concentration of 1% to one of the replicate cultures. All samples were then incubated at

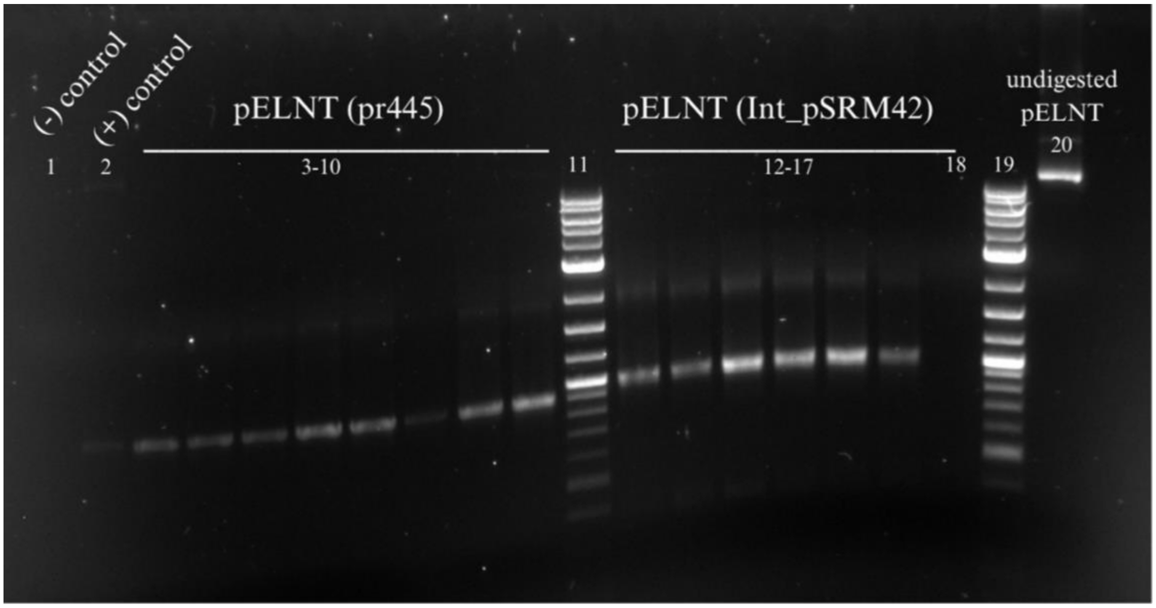

Figure 3.4. PCR of pELNT plasmids isolated from *P. syringae* GR12-2 (amplified with NT_F and pr445 primers (expected 859 bp band, lanes 3-10) or int_pSRM42 and pr445 primers (expected 960 bp band, lanes 12-17)), with a negative pELNT PCR control (lane 1), a positive control of pELNT from previous colony PCR (lane 2), undigested pELNT (lane 20) and 2-log DNA ladder as the marker (lanes 11 and 19).

27°C for another two hours. Samples were spun down, the supernatants were discarded, and the cell pellets were frozen at -20°C.

Frozen pellets were resuspended in 200 μl of 0.85% NaCl and sonicated to clarity on ice. A Bradford assay was performed to determine protein concentration (Bradford, 1976). Ten μg of each sample grown with or without L-arabinose was mixed with Laemmli sample buffer (Bio-Rad #1610747) containing dithiothreitol (DTT; Sigma #43816) and heated at 95°C for five minutes. Samples were then loaded into two 14% SDS-polyacrylamide gels (30% Acrylamide/Bis solution 37.5:1 (BioRad #1610158), 10% sodium dodecyl sulfate (SDS), 10% ammonium persulfate, tetramethylethylenediamine (TEMED), 1.5M Tris-HCL pH 8.8 for resolving gel and 0.5M Tris-HCL pH 6.8 for stacking gel). Gels were run at 140 V for one hour and 15 minutes. One gel was stained with Biosafe Coomassie Blue and de-stained in water before imaging. The second gel was equilibrated for 30 minutes in the transfer buffer (Tris/glycine/SDS buffer (BioRad #1610732), methanol, and water). A transfer sandwich consisting of transfer buffer-soaked extra-thick filter paper (BioRad #1703959), an Immuno-Blot PVDF membrane (Bio-Rad #162-0174; presoaked in methanol), the equilibrated gel, and another sheet of buffer-soaked filter paper were placed in a Trans-Blot Semi-Dry Electrophoretic Transfer Cell (Bio-Rad #170-3940). The transfer was completed at 25 V and 1 A for 30 minutes. The membrane was then blocked in Tween-20 Tris-buffered saline (TTBS; 20 mM Tris-HCL (pH 7.5), 500 mM NaCl, 0.05% Tween 20) with 3% skim milk (Thermo Scientific #LP0033B) for two hours. TTBS with 1.5% skim milk and anti-FLAG rabbit polyclonal antibody (Sigma #F7425, 1:3000d) was applied to the membrane overnight at room temperature. The next day, the membrane was washed in TTBS for five minutes in triplicate, with a final five minute wash in Tris-buffered saline (TBS; 20 mM Tris-HCL (pH 7.5), 500 mM NaCl). The membrane was then incubated for two hours in TTBS with 1.5% skim milk and anti-rabbit IgG conjugated alkaline phosphatase goat polyclonal antibody (Sigma #A3687, 1:3000d). The previous washing steps were repeated, and the membrane was incubated for 10 minutes in color developer using the AP Conjugate Substrate Kit (Bio-Rad #1706432).

Optimization of fusion protein expression and biotinylation

Three ml of LB broth with four μg/ml tetracycline were inoculated with J253 and J257 strains (Table 3.1) in triplicate and grown at 27°C overnight. Cultures were centrifuged, washed three times and resuspended in 1.5 ml of 1X minimal (M9) salts. The resuspension was used to inoculate 50 ml of M9G and four μg/ml tetracycline broth to an OD_{600nm} of 0.05. The cultures were grown to an OD_{600nm} of ~0.6-0.8 and then treated with 0.01% L-arabinose, 0.01% L-arabinose and 50 μM biotin, or left untreated, and incubated at 27°C. Samples (1.5 ml) were collected at 2, 4, 6, 8, 20, and 24 hours post-induction, and cell pellets were frozen at -20°C.

To determine optimal induction time, frozen cell pellets were thawed, resuspended in 200 μl of 0.85% NaCl, and sonicated to clarity on ice. A Bradford assay was performed to determine protein concentration (Bradford, 1976). Ten μg of each sample with and without 0.01% L-arabinose were mixed with Laemmli buffer containing DTT, heated at 95°C for five minutes, and then loaded into two 14% SDS-polyacrylamide gels. Gels were run at 140 V for one hour and 10 minutes, and then anti-FLAG Western blots were performed as described above.

To assess protein biotinylation, a streptavidin-HRP Western blot was performed. Frozen pellets of cells grown with 0.01% L-arabinose with or without 50 µM biotin for 2, 4, 6, 8, 20, and 24 hours were thawed, resuspended in 200 µl of 0.85% NaCl, and sonicated to clarity on ice. A 100 µl aliquot of each sample was centrifuged at 13,000 RPM for five minutes. The supernatant was transferred to a new tube, and a Bradford assay was done to determine protein concentration (Bradford, 1976). Ten µg of each sample was added to Laemmli sample buffer with DTT, then heated at 95°C for five minutes. Heated samples and 10 µl of Precision Plus Protein All Blue Standards (Bio-Rad #1610373) were loaded into 14% SDS-polyacrylamide gels and ran at 140 V for one hour and 30 minutes. One set of gels was stained using Biosafe Coomassie and de-stained in water, while the other set of gels was equilibrated in transfer buffer for 30 minutes. Transfer sandwiches were assembled with transfer buffer-soaked extra-thick filter paper, a methanol-treated PVDF membrane, the equilibrated gel, and another sheet of soaked filter paper in the Trans-Blot semi-dry transfer cell. The transfer was done at 25 V and 1 A for 30 minutes. The PVDF membranes were blocked in TTBS with 5% bovine serum albumin (BSA; Sigma, MO, USA) on a shaker overnight. The following day, the membranes were washed three times in TTBS for five minutes, with a final wash in TBS for five minutes. TTBS with 2.5% BSA and horseradish peroxidase-conjugated streptavidin (Thermo Scientific #N100, 1:3000d) was applied to the membrane for two hours and was followed by repeating the previous washes. The membranes were developed using Pierce™ ECL Western Blotting Substrate (Thermo Scientific #32209) and imaged using the Chemidoc MP (BioRad).

Affinity purification of biotinylated proteins

Single colonies of strains J251, J253, J254, and J257 were inoculated into three ml of LB broth with four μg/ml tetracycline and grown for ~12 hours at 27°C. Cells were then pelleted and washed three times in 1X M9 salts. Pellets were resuspended in 1X M9 salts and were used to inoculate 20 ml of M9G broth with four μg/ml tetracycline to an OD_{600nm} of 0.05. Cultures were grown at 27°C until an OD_{600nm} of ~0.6-0.8 was reached. Biotin was added to a final concentration of 50 μM and incubated at 27°C for 20 hours. After the 20-hour incubation, 15 ml of the cultures were centrifuged, and the cell pellets were washed three times in PBS (phosphate-buffered saline (pH 7.4)) and stored at -80°C.

To capture biotinylated proteins, 50 μl of Dynabeads MyOne Streptavidin C1 beads (Invitrogen #65001) was withdrawn from the stock bottle and captured on magnets (Qiagen #36912) for two minutes. The supernatant was discarded, and the beads were washed three times in 0.5 ml PBST (phosphate-buffered saline (pH 7.4), 0.1% Tween 80) and then resuspended in the original bead volume plus 10 μl per 100 μl bead volume of PBST. To confirm the self-biotinylation of the $BirA^{R55G}$-TPR fusion proteins, and to perhaps visualize biotinylated interacting proteins, FLAG-tagged fusion proteins were affinity purified by anti-FLAG tag magnetic beads and assessed in a streptavidin-HRP

Western blot. Anti-FLAG M2 Magnetic Beads (40 μl per sample; Sigma-Aldrich #M8823) were prepared and added to resuspended cell pellets as described above.

Frozen pellets were thawed, resuspended in one ml PBS, and sonicated to clarity on ice. The sonicated cultures were centrifuged, the pellet discarded and the supernatant moved to a new tube in preparation for the magnetic beads. The supernatant samples were supplemented with 10 μl of 10% Tween 80 (Sigma-Aldrich #P8074). For affinity purification using streptavidin beads, 50 μl of the prepped beads were added to each sample, and rotated at room temperature for 20 minutes. For affinity purification using anti-FLAG beads, 40 μl of the prepped beads were added to each sample, and rotated at room temperature for 30 minutes. After incubation, the beads were captured by magnets for two minutes, and washed three times in one ml PBST. During the final wash, 100 μl of bead/lysate suspension was removed and transferred to new 1.5 ml tube for protein gels. Remaining beads were frozen at -20°C.

The 100 μl aliquot of the bead/lysate solution was captured on magnets for 20 mins after adding 400 μl PBST. The supernatant was discarded, and the beads were resuspended in 25 μl of 2X biotin-saturated Laemmli buffer (one ml 4X Laemmli Sample Buffer (Bio-Rad), one ml of 0.2mg/ml biotin) and supplemented with PBST to a final volume of 50 μl. The samples were heated at 70°C for 15 minutes. From this stage, the protocol written above for streptavidin-HRP Western was repeated to visualize affinity purified proteins.

Optimization of fusion protein expression and biotinylation

An initial Western blot was done to confirm the expression of the BirA^{R55G}-T3SS fusion proteins in *P. syringae* strains by immunoblotting using an anti-FLAG antibody to detect the FLAG tag. Expression of fusion proteins are evidenced by bands of the expected size in strains J251 and J254 carrying C- and N- terminal *birA^{R55G}-hrcN* fusions, respectively, (77 kDa), in strain J252 carrying a C-terminal *birA^{R55G}-hrcV* fusion (107 kDa), and in strains J253 and J256 carrying C- and N-terminal *birA^{R55G}-TPR* fusions, respectively, (57 kDa) (Figure 3.5). Unexpected bands were observed for strains J253 (~150 kDa) and J256 (~28 kDa). The positive control strain J257, which expresses only the BirA^{R55G}-FLAG fusion (28 kDa), yielded a band of the expected size. L-arabinose increased the expression of the fusion proteins compared to those without induction, however, L-arabinose appears to be unnecessary for fusion protein expression.

A second anti-FLAG Western blot was performed to determine the optimal time of L-arabinose induction for expression of BirA^{R55G}-T3SS fusion proteins in M9G minimal medium. Proteins from strains J253 and J257 yielded expected bands of 57 kDa and 28 kDa, respectively, of more or less equal intensity at all time points (Figure 3.6). L-arabinose had a minimal effect on fusion protein expression in M9G medium, with only a slight increase in expression between induced and uninduced samples. These results confirm that L-arabinose is not necessary to induce fusion protein expression in *P. syringae* GR12-2.

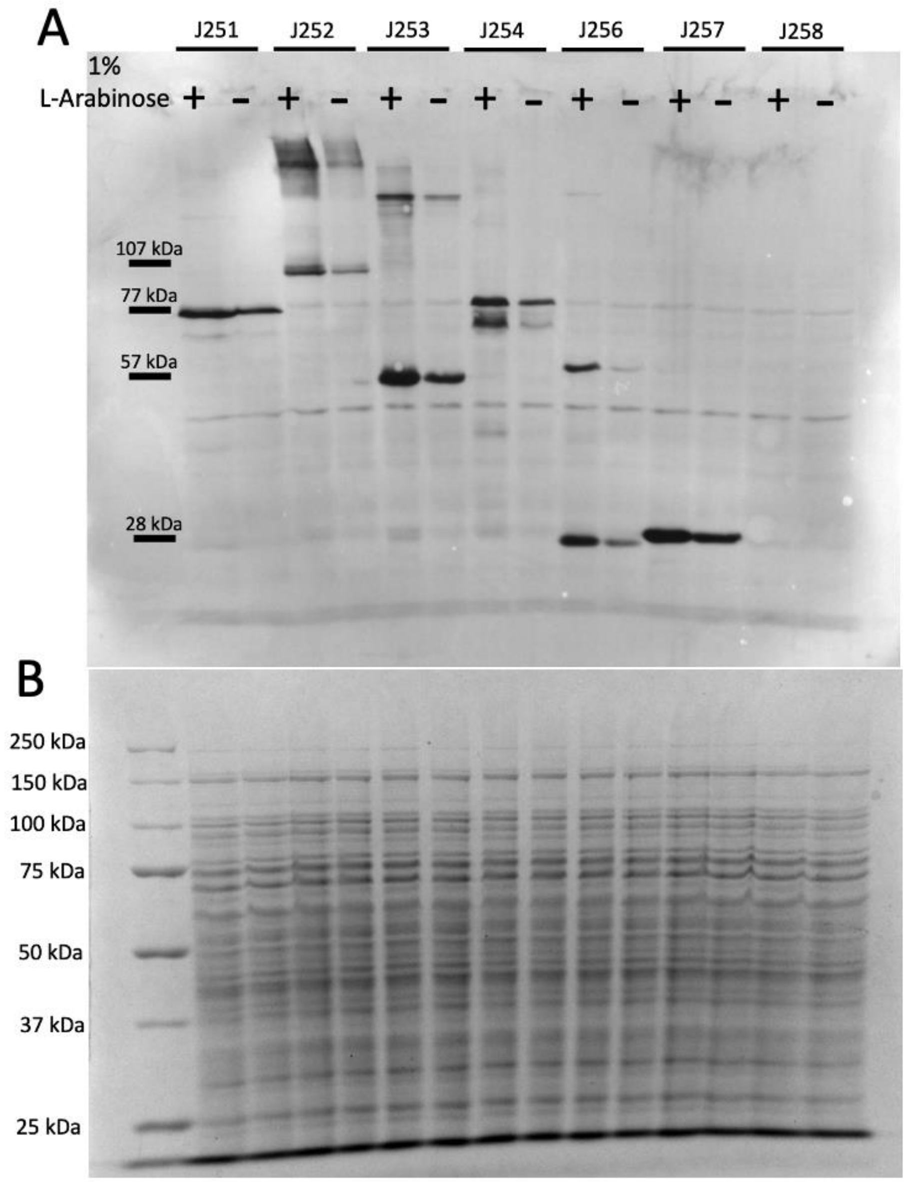

Figure 3.5. A) Anti-FLAG Western Blot confirming expression of *birA*^{R55G}*-T3SS* fusions in strains J251, J252, J253, J254, J256, and J257 grown in LB and uninduced or induced with L-arabinose (1%) for 2 h. Proteins from *P. syringae* J258, which carries pHERD26T without the *birA*^{R55G}*-FLAG* fusion, was included as a negative control. B) Samples in the same order were run on a 14% SDS-PAGE gel stained with Biosafe Coomassie Blue.

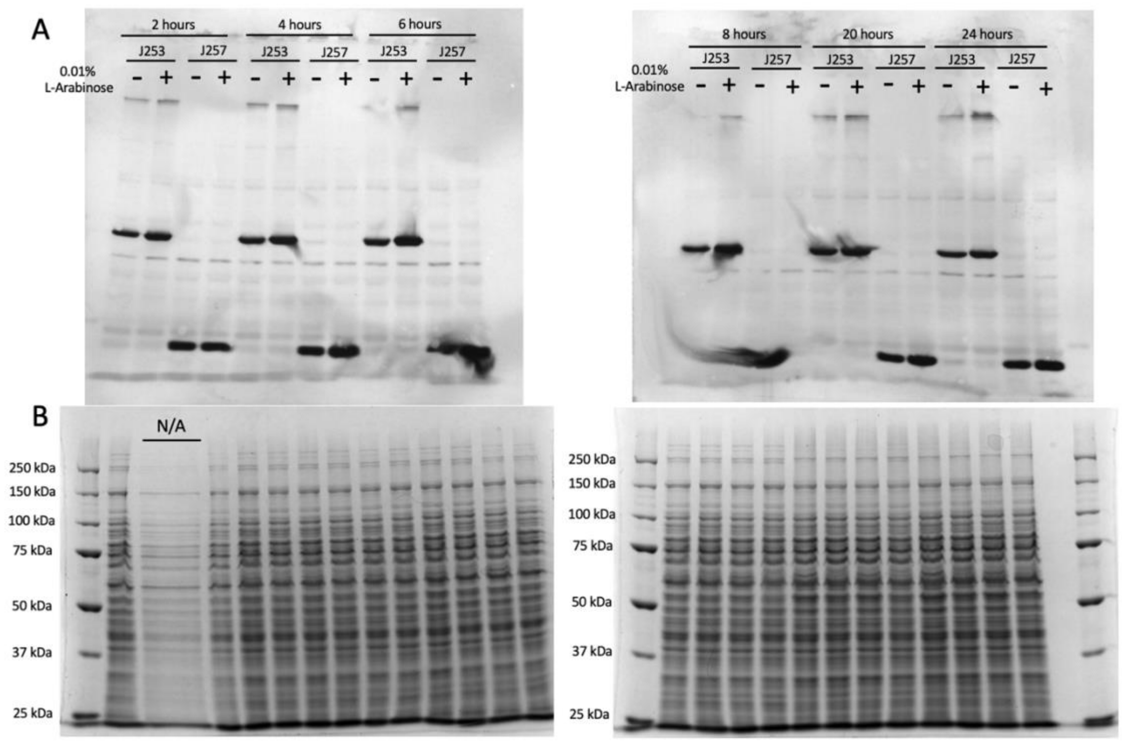

Figure 3.6. A) Anti-FLAG Western blots to assess induction with L-arabinose of J253 and J257 grown in 1X M9G with 4 μg/ml tetracycline, with or without a 2-hour L-arabinose induction (final concentration = 0.01%) sampled at 2, 4, 6, 8, 20, or 24 hours. L-arabinose induction was unnecessary for expression of FLAG-tagged fusion proteins. B) Samples in the same order were run on a 14% SDS-PAGE gel stained with Biosafe Coomassie Blue.

A streptavidin-HRP Western blot was done to determine the incubation time of biotin supplementation required to visualize biotinylation from protein interactions with the BirA^{R55G}-T3SS fusion proteins. Strains of J253 and J257 induced with 0.01% L-arabinose, and incubated with or without 50 µM biotin at all time points showed an intense band at ~65-70 kDa, and at <25 kDa (Figure 3.7). A 28 kDa band was also seen in the samples from control strain J257 that were treated with 0.01% L-arabinose and 50 µM biotin, with increasing intensity over the time points. The 28 kDa bands were expected for this strain as BirA^{R55G} is known to self-biotinylate (Choi-Rhee *et al.*, 2008). No bands indicative of self-biotinylation by the fusion protein expressed in J253 (57 kDa) were observed, possibly due to low abundance. The results of this Western blot indicate that 50 µM of biotin is sufficient and necessary to promote biotinylation by the heterologous BirA^{R55G} and that a longer incubation time of 20 hours increases biotinylation.

Affinity purification of biotinylated proteins

To identify effector proteins, proteins that interacted with a BirA^{R55G}-T3SS fusion protein were subsequently biotinylated and were captured by affinity purification with streptavidin-linked magnetic beads. Before sending captured proteins for identification by MS, a streptavidin-HRP Western blot was performed to assess the biotinylated proteins. The streptavidin-HRP blot showed biotinylated proteins at ~65-70 kDa and <25 kDa among the captured proteins from all strains, including the control strain which does not possess a BirA^{R55G}-T3SS fusion protein, suggesting that the proteins in these bands are

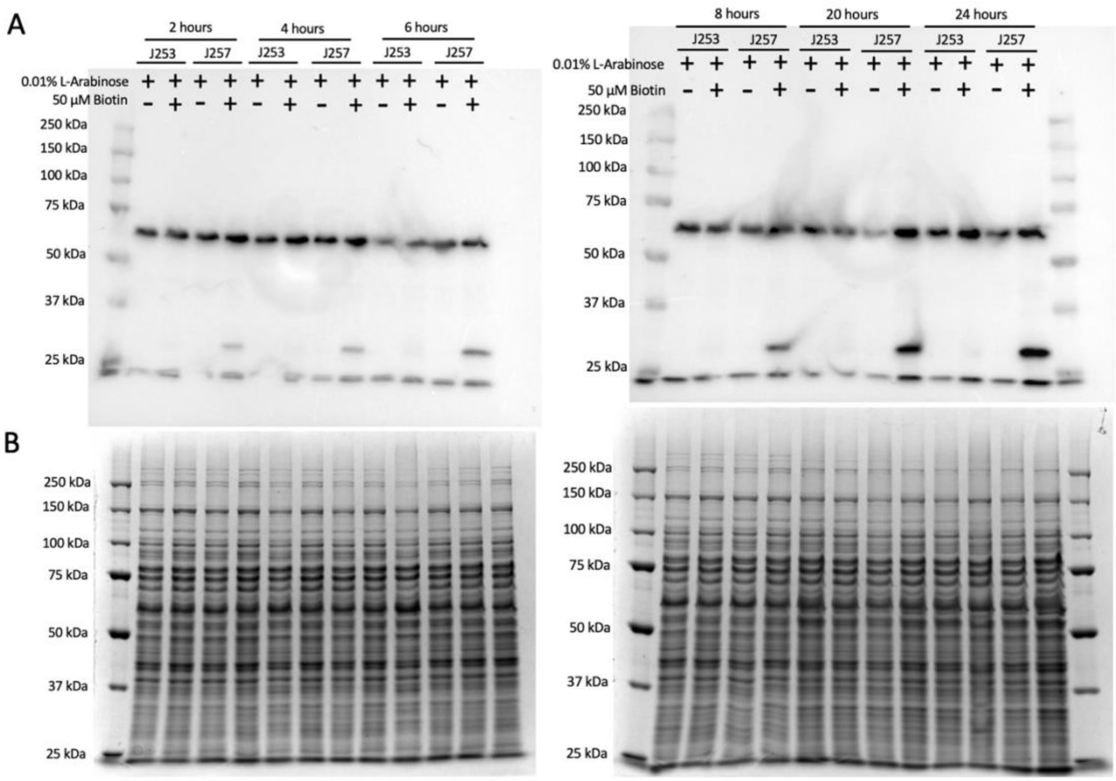

Figure 3.7. A) Streptavidin-HRP Western blot to assess biotin supplementation of J253 and J257 cultures grown in M9G with 4 μg/ml tetracycline and 0.01 % L-arabinose induction, with or without 50 μM biotin sampled at 2, 4, 6, 8, 20, or 24 hours. Increased length of supplementation results in higher expression of fusion proteins. B) Samples in the same order were run on a 14% SDS-PAGE gel stained with Biosafe Coomassie Blue. The blot and gel were loaded with Precision Plus Protein All Blue Standards (Bio-Rad #1610373) as a marker.

biotinylated independently of T3SS-interaction, possibly by an endogenous protein (Figure 3.8A). Similar bands at ~65-70 kDa and <25 kDa were also seen in the polyacrylamide gel (Figure 3.8B). In repeat assays, an intense 65-70 kDa band dominated, obscuring assessment of proteins biotinylated via interaction with the fusion proteins (data not shown). Considering this and a lack of evidence for the expected self-biotinylation of the $BirA^{R55G}$-T3SS fusion proteins, the affinity-purified samples were not processed further.

Proteins captured by the anti-FLAG M2 Magnetic Beads were assessed in a streptavidin-HRP Western blot. Biotinylated proteins were seen at ~57 kDa in proteins captured from J253 culture lysates and at ~28 kDa in those from J257, as expected for the self-biotinylated $BirA^{R55G}$-TPR fusion protein and for $BirA^{R55G}$ in the control, respectively (Figure 3.9). The endogenously biotinylated protein at ~65-70 kDa is also present in all samples, and interestingly, a potential biotinylated protein around ~75 kDa from the J253 strain. These results indicate that the captured FLAG-tagged fusion proteins are indeed biotinylated, and although biotinylated, most interacting proteins were not apparent in the Western blot.

Discussion

This study attempted to identify effectors secreted by the T3SS using proximity-dependent protein biotinylation. Proteins that interacted with fusions of $BirA^{R55G}$ and T3SS proteins would be biotinylated by $BirA^{R55G}$ and affinity purified using streptavidin-conjugated beads for identification by MS. C- and N-terminal $BirA^{R55G}$ fusions with

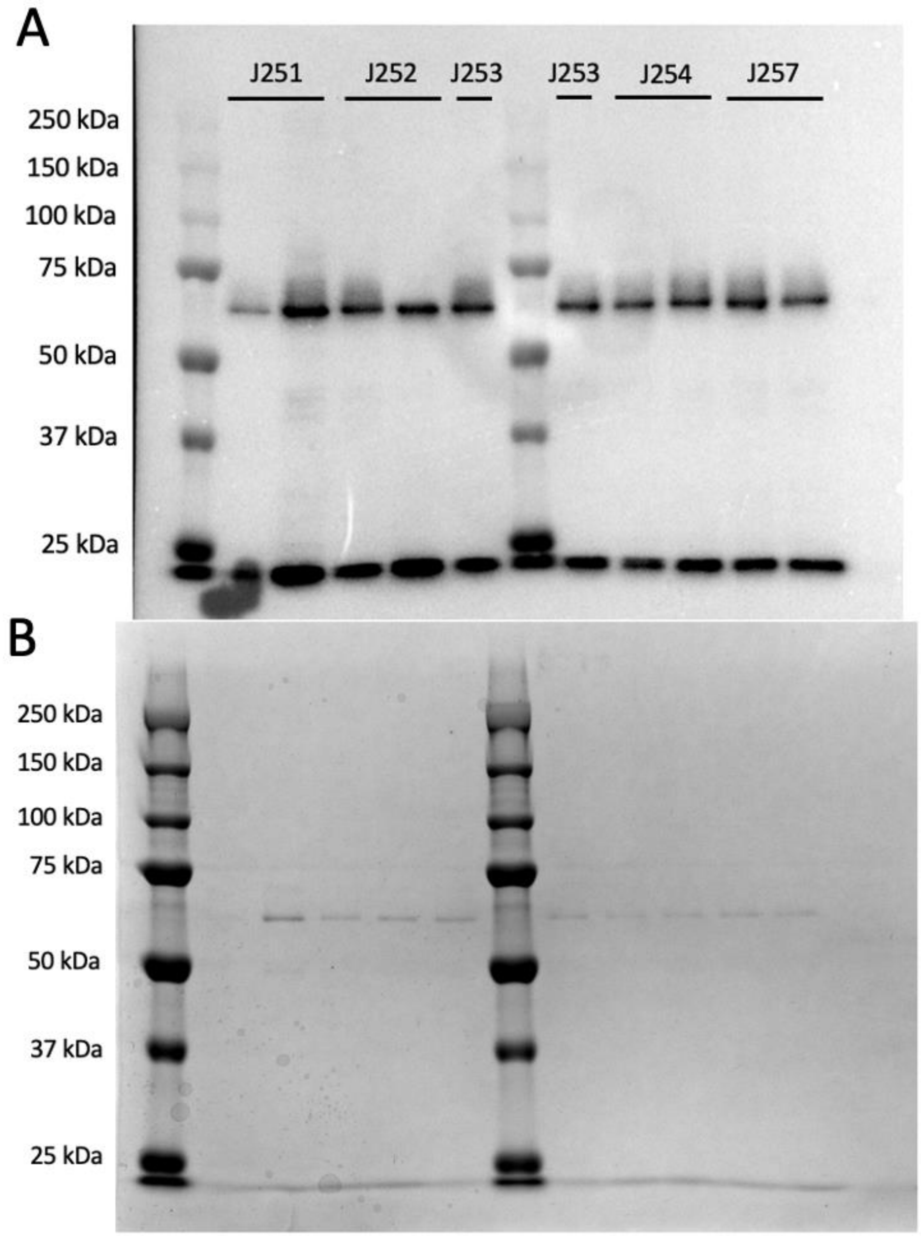

Figure 3.8. Affinity purification of biotinylated proteins with streptavidin-conjugated beads. A) Streptavidin-HRP Western blot of proteins in duplicate culture lysates of J251, J252, J253, J254 and J257 grown in M9G with 4 μg/ml tetracycline and 50 μM biotin captured with streptavidin-linked magnetic beads. B) Samples in the same order were run on a 14% SDS-PAGE gel stained with Biosafe Coomassie Blue. The blot and gel were loaded with Precision Plus Protein All Blue Standards (Bio-Rad #1610373) as a marker.

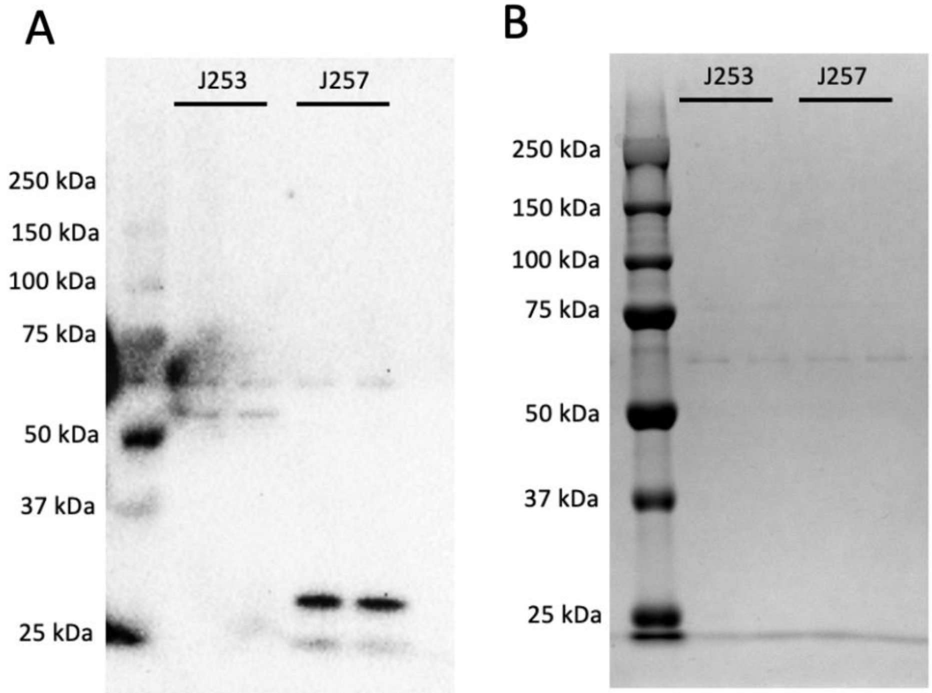

Figure 3.9. Affinity purification of biotinylated proteins with streptavidin- or anti-FLAG antibody-conjugated beads. A) Streptavidin-HRP Western blot of proteins in culture lysates of strains J251, J253, J254, and J257 grown in M9G with 4 μg/ml tetracycline and 50 µM biotin and captured with either streptavidin- or anti-FLAG antibody-linked magnetic beads B) Samples in the same order were run on a 14% SDS-PAGE gel stained with Biosafe Coomassie Blue. The blot and gel were loaded with Precision Plus Protein All Blue Standards (Bio-Rad #1610373) as a marker.

HrcV, HrcN, or a predicted TPR motif-containing chaperone were successfully generated, with the exception of the N-terminal BirA^{R55G}-HrcV fusion. Despite multiple attempts, *hrcV* could not be inserted into pSRM42.

An anti-FLAG Western blot to confirm expression of the fusion proteins showed bands at the expected fusion protein sizes, indicating correct expression of all fusion proteins. However, additional bands were seen in several strains. A FLAG-tagged 28 kDa band produced by strain J256 is consistent with the expected size of BirA^{R55G-}-FLAG. This indicates that some of the fusion protein is degraded, cleaving off BirA^{R55G}. The incomplete degradation could be caused by the creation of the fusion protein inadvertently generating a site for proteolytic cleavage.

Western blots were also performed to determine the concentration of L-arabinose to use for induction of the *birA^{R55G}-T3SS* fusions from the arabinose-inducible *araBAD* promoter (Qiu *et al.,* 2008b). Results from an initial anti-FLAG Western blot of proteins from a culture in LB medium with a final concentration of 1% L-arabinose showed that arabinose is not required for fusion protein expression, although expression was higher in induced compared to uninduced cultures. In subsequent cultures in M9G medium, a final concentration of 0.01% L-arabinose was used as several papers showed successful arabinose induction in *Pseudomonas* species using a lower L-arabinose final concentration (Cook *et al.,* 2018; Qiu *et al.,* 2008a). Judging from the intensities of bands in a Western blot, there was no apparent difference in expression of the fusion proteins between induced and uninduced cultures leading to the conclusion that addition of L-arabinose was not necessary for fusion protein expression in M9G medium. Constitutive expression from the *araBAD* promoter has also been seen in studies using *P. aeruginosa* (Meisner & Goldberg, 2016; Williams McMackin *et al.*, 2021).

The *E. coli araBAD* promoter uses two mechanisms for maximum expression. The first is the binding of L-arabinose to the AraC transcription factor. In the absence of arabinose, AraC binds to the *araBAD* promoter acting as a repressor to reduce expression of the *araBAD* operon (Guzman *et al.,* 1995) Upon binding to L-arabinose, the conformation of the AraC dimer changes and it binds to the *araBAD* promoter such that it activates high levels of expression. *P. syringae* GR12-2 does not possess an *araBAD* operon or the *araC* gene encoding AraC, however, *araC* is present on the pHERD26T vector (Qiu *et al.,* 2008b), from which the fusion proteins are expressed in this study and therefore arabinose supplementation was expected to increase fusion protein expression. The second mechanism for control of the *araBAD* promoter is the availability of glucose in the growth medium. In *E. coli,* in the absence of glucose, cyclic AMP (cAMP) binds to the cAMP-catabolite repressor protein (CRP) to activate expression of the *araBAD* operon (Guzman *et al.,* 1995; Hahn *et al.,* 1984; Williams McMackin *et al.,* 2021), *Pseudomonas* spp. possess CRP family proteins (Thomas *et al.,* 2021; Winsor *et al.,* 2015), however, they differ from *E. coli* in that cAMP levels do not fluctuate in the presence or absence of glucose and they do not utilize cAMP-CRP carbon catabolite repression (Rojo, 2010). Therefore, the constitutive expression of the BirA^{R55G}-T3SS fusion proteins in *P. syringae* GR12-2, especially in M9G medium, might be attributed to the lack of carbon catabolite repression.

Affinity purification of biotinylated proteins using streptavidin-linked magnetic beads was assessed by performing a streptavidin-HRP Western blot. Proteins captured using the streptavidin-linked beads that were interacting, strongly or transiently, with the BirA^{R55G}-T3SS fusions could not be seen on Western blots. However, ubiquitous bands of ~65-70 kDa and <25 kDa biotinylated proteins were seen among the proteins captured from all strains, including control strains that do not express a fusion protein, suggesting that they are biotinylated by an enzyme that is native to *P. syringae* GR12-2. BioID was first constructed using a mutated variant of a biotin protein ligase from *E. coli,* which natively biotinylates a single protein, the biotin carboxyl carrier protein (Choi-Rhee *et al*., 2008; Fall *et al.,* 1975). However, *E. coli* and *Pseudomonas* exhibit differences in their biotin requirements and in their biotinylation enzymes. Compared *to E. coli*, *P. aeruginosa* has 3-fold more cytosolic biotin and physiologically requires >10-fold more biotin than *E. coli* (Shi *et al*., 2023). This is logical when considering that *P. aeruginosa* is predicted to have five enzymes that require biotin, while *E. coli* only has one, BirA. The predicted biotin-requiring enzymes in *P. aeruginosa* are carboxylases involved in the tricarboxylic acid cycle (Best & Knauf, 1993; Kaschani *et al.,* 2016; Satiaputra *et al.,* 2016; Shi *et al.*, 2023). Of the predicted *P. aeruginosa* biotinylated proteins, four have a molecular weight similar to those of the ubiquitous biotinylated proteins captured by the streptavidin-conjugated beads, and have orthologues in *P. syringae* GR12-2 (Winsor *et al.,* 2015). These are methylcrotonyl-CoA carboxylase α-subunit (70.7 kDa), which shares 72% identity with the protein encoded by AFK24_28780 in *P. syringae* GR12-2; geranyl-CoA carboxylase α-subunit (71.1 kDa), which shares 65.1% identity with the protein encoded by AFK24_27870; pyruvate carboxylase subunit B (65.7 kDa), which shares 85.9% identity with the protein encoded by AFK24_07675, and acetyl-CoA carboxylase biotin carboxyl carrier protein (16.1 kDa), which shares 76.9% identity with the protein encoded by AFK24_03140. Thus, the abundant affinity-purified proteins are likely proteins that are naturally biotinylated by *P. syringae* GR12-2 enzymes, independently of the T3SS.

The abundant naturally biotinylated proteins may outcompete and thereby reduce biotinylation and/or capture of proteins that are biotinylated from interaction with the fusion proteins. Given the lack of evidence for affinity-purification of the latter proteins, the samples were not analyzed further by MS. Alternative affinity purification methods to capture interacting protein in *Pseudomonas* should be considered. A preliminary experiment conducted here suggests that affinity purification of the FLAG-tagged TPR protein was successful, however, it may be less effective for detecting transient or weaker interactions which are expected for effectors that interact with T3SS. This study has shown that, in *P. syringae* GR12-2, proximity-dependent biotinylation has obstacles that will need to be overcome for effective use in identifying protein interactions.

Chapter 4: Identification of Proteins that Interact with a T3SS Chaperone Using Affinity Purification

Introduction

Another approach to determine the function of the T3SS in *P. syringae* GR12-2 and identify secreted effector proteins is to detect proteins that interact with T3SS chaperones by affinity purification. Chaperones are essential for effector secretion and are divided into three classes based on the substrates they interact with and when those substrates are secreted. Chaperones that interact with early substrates are in Class II, those that interact with middle substrates are in Class III, and those with late substrates are in Class I (Izoré *et al.,* 2011; Portaliou *et al.,* 2016). All function in the cytoplasm to stabilize proteins, to prevent inappropriate effector interactions before secretion, and to maintain the protein substrates in a secretion-competent state (Alfano & Collmer, 2004; Page & Parsot, 2002). Chaperones form a complex with their effectors and target them to the secretion apparatus which recognizes the complexes. The recognition of the chaperone-effector complexes facilitates hierarchy and competition in secretion (Alfano & Collmer, 2004; Page & Parsot, 2002; Portaliou *et al.,* 2016). In addition to being necessary for the secretion of effectors into host cells or the extracellular medium, chaperones play a role in the regulation of the T3SS (Feldman & Cornelis, 2003; Izoré *et al.,* 2011; Portaliou *et al.,* 2016).

Class II and III chaperones typically contain three TPR motifs (Pallen *et al.,* 2003). TPR motifs are tetracopeptide repeats that form superhelical structures when present in triplicate, suited for mediating protein interactions and transport (Cerveny *et al.,* 2013; Izoré *et al.*, 2011; Page & Parsot, 2002). The TPR-containing protein encoded by AFK24_20305, was predicted to be a chaperone due to three TPR motifs in its sequence (Stocek, 2018). If the TPR-containing protein is indeed a T3SS class II or III chaperone, proteins associated with the T3SS can be identified based on their interaction with the predicted chaperone.

Affinity purification may be used to capture and identify proteins that interact with the predicted TPR chaperone. Affinity purification allows for the isolation of proteins that carry a specific peptide sequence (affinity tag) that selectively binds to a ligand and thereby can be separated out of a complex mixture. Ligands, such as antibodies or enzymes, are immobilized on a support and are then exposed to a complex mixture of proteins. Proteins bound selectively to the binding agent are then eluted from the binding agent (Rodriguez *et al.,* 2020).

In the construction of the *birA^{R55G}-T3SS* fusions, (see Chapter 3, Figure 3.1), an eight-amino acid FLAG tag was included adjacent to *birA^{R55G}* to confirm fusion protein expression in Western blots using an anti-FLAG antibody. The FLAG tag was later exploited to capture the TPR chaperone-BirA^{R55G} fusion proteins by affinity purification with anti-FLAG antibody-linked magnetic beads to detect their self-biotinylation in a streptavidin-HRP Western blot. Exploiting the FLAG tag to capture the TPR chaperone-BirA^{R55G} fusion protein together with any proteins that interact with it may offer another method to achieve the objective of this study, which is to further determine the function of the T3SS in *P. syringae* GR12-2 by identifying proteins that it secretes.

Methods

Bacterial culture conditions

Colonies of *P. syringae* J253, J256, and J257 strains (Table 4.1) were inoculated into three ml of M9G with four μg/ml tetracycline in duplicate and grown overnight at 27°C. Then, overnight cultures were inoculated into 20 ml of M9G broth with four μg/ml tetracycline to an OD_{600nm} of 0.05. Cultures were grown at 27°C until an OD_{600nm} of ~0.6-0.8 was reached (approximately 13 hours). Fifteen ml of the cultures were centrifuged (4000 RPM at 4°C for 20 minutes), and the cell pellets were washed with one ml PBS, pH 7.4, repelleted, and then stored at -20°C.

Affinity purification using anti-FLAG magnetic beads

Cell pellets were thawed and resuspended in one ml TBS supplemented with Protease Inhibitor Cocktail (Sigma #P-2714, d1:100). The cell suspensions were then sonicated to clarity on ice, centrifuged briefly to remove debris, and the cell lysate supernatant was collected. The supernatant was supplemented with 10 μl of 10% Tween

Table 4.1. *Pseudomonas syringae* GR12-2 derivatives used in this section of the study.

Strain	*P. syringae* background	Plasmid	Gene of Interest	Source
J253	GR12-2	pEJCT	*TPR* chaperone	Jong, unpublished
J256	GR12-2	pELNT	*TPR* chaperone	This study
J257	GR12-2	pSRM43	$birA^{R55G}$	Jong, unpublished

80 and 40 μl of anti-FLAG magnetic beads that were prepared as follows. A volume of 40 μl per sample of anti-FLAG M2 Magnetic Beads (Sigma-Aldrich #M8823) was withdrawn from the stock bottle, captured with a magnet for two minutes, and the supernatant was discarded. The beads were washed in 10 times their volume in TBS and resuspended in TBS to the original volume withdrawn.

The cell lysates were incubated with the prepared anti-FLAG M2 magnetic beads for four hours at room temperature with slow rotation. After the incubation period, the anti-FLAG beads were captured with a magnet for two minutes, the supernatant was discarded, and the beads were washed three times in one ml TBS. During the final wash, a 100 μl aliquot of the bead/lysate suspension was removed for the protein gel/Western blot. The remaining beads were washed in one ml ammonium bicarbonate (50 mM) three times and stored at -20°C for MS.

Mass spectrometry of proteins

Duplicate frozen samples of the affinity-purified proteins were sent on dry ice to the Proteomics Platform of the Centre Hospitalier Universitaire de Quebec Research Center (Laval, Quebec, Canada) for LC/MS/MS analysis. Each set of replicates underwent a separate LC/MS/MS run. Samples underwent tryptic digestion and were loaded into the Dionex Ultimate 3000 nanaRSLC chromatography system (Thermo Fisher Scientific) with a nanoelectrospray ion source. Samples were separated on a 75 µm x 50 cm PepMax RSLC EASY-Spray column (Thermo Fisher Scientific). The Orbitrap Fusion Tribrid mass spectrometer (Thermo Fisher Scientific) obtained mass spectra via an initial MS scan, followed by data-dependent MS/MS scans of the most intense ions.

Mass spectrometry data analysis parameters

Tandem MS data files were generated by Proteome Discoverer 2.3 software (Thermo Fisher Scientific) and analyzed using Mascot (Matrix Science, London, UK; version 2.5.1; Perkins *et al.,* 1999). Uniprot *Pseudomonas syringae* (5674 entries, UP000093104; Patten *et al.*, 2016) was the database against which the MS/MS data was searched, assuming tryptic digestion. Mascot searched the database with the parameters of a 0.60 Da fragment ion mass error tolerance and a parent ion mass error tolerance of 10 PPM. The fixed modification of carbamidomethylation of cysteine and variable modifications, including oxidation of methionine and deamidation of asparagine and glutamine, were set for Mascot.

Scaffold (version 4.8.4, Proteome Software Inc., Portland, OR) was used to visualize and compile MS data. Scaffold was used to validate the peptide and protein identifications from the MS/MS data. Scaffold uses the Protein Prophet algorithm to assign probabilities that the proteins were correctly identified, and a minimum probability of 99.9% was used (Nesvizhskii *et al.*, 2003). Proteins must also have five unique peptides identified to meet stringent thresholds. For this data, a minimum peptide threshold of 95% was used, and correct peptide identification was determined by the Scaffold Local False Discovery Rate algorithm (Searle, 2010). Proteins were sorted and filtered using total spectrum counts, which are all the identified spectra associated with each protein, unique or shared among other proteins.

Results

MS analysis of proteins captured by affinity purification of FLAG-tagged fusion proteins produced by *P. syringae* strains J253, J256, and J257, identified a total of 270 unique proteins in the first LC/MS/MS run for one set of replicates (Figure 4.1). Twelve proteins were present exclusively in the sample from the J253 strain, and three were present exclusively in the sample from the J256 strain. Four proteins were present among the proteins pulled down from both J253 and J256 but absent in those from the control strain J257. The remaining 233 proteins were captured by affinity purification from all three cultures. In the second LC/MS/MS run for the second set of replicates, 230 unique proteins were identified in total, with 225 proteins found in samples from J253, J256 and J257 (Figure 4.2). Three of the remaining five proteins were present among the proteins from both J253 and J256, and two were found exclusively in J253. All proteins considered further had a minimum total spectrum count of five in at least one of the cultures expressing the FLAG-tagged TPR fusion protein.

Of greatest interest in this study are proteins that are reproducibly present among the those affinity-purified with both the C- and N-terminal FLAG-tagged TPR chaperone fusions and absent among those from the control strain, J257. Only one protein, the TPR

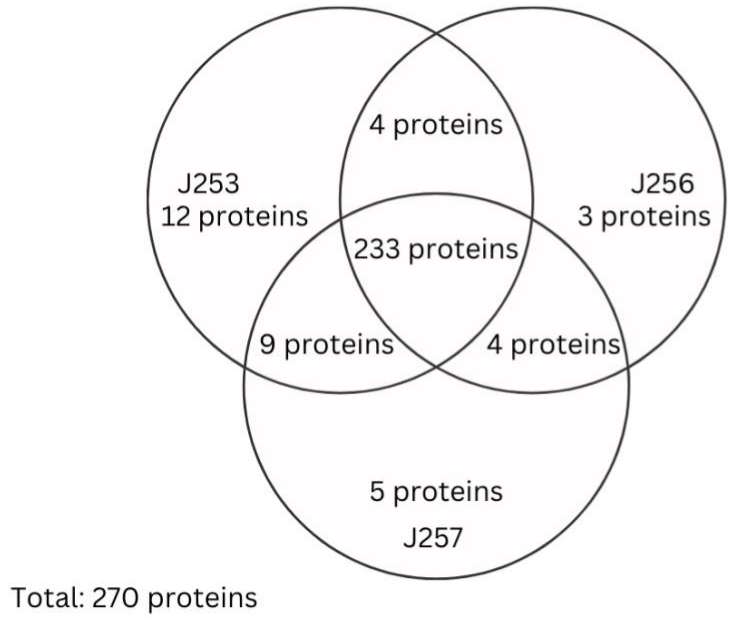

Figure 4.1. A total of 270 unique affinity-purified proteins were identified from anti-FLAG linked magnetic beads incubated in cultures of *P. syringae* strains J253, J256 and J257. The proteins are from the first dataset identified by LC/MS/MS (protein threshold, 99.9%; peptide threshold, 95%; minimum of 5 peptides). The Venn diagram displays the composition of proteins found in each sample.

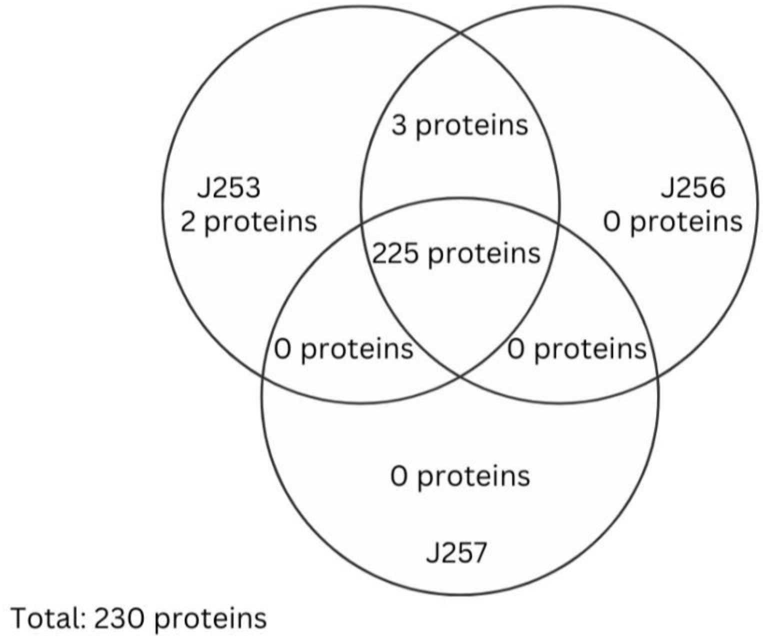

Figure 4.2. A total of 230 unique affinity purified proteins were identified from anti-FLAG linked magnetic beads incubated in cultures of *P. syringae* strains J253, J256 and J257. The proteins are from the second dataset identified by LC/MS/MS (protein threshold, 99.9%; peptide threshold, 95%; minimum of 5 peptides). The Venn diagram displays the composition of proteins found in each sample.

chaperone bait protein itself, met this criteria (Table 4.2). Pyridine nucleotide-disulfide oxidoreductase and 4-hydroxy-tetrahydrodipicolinate synthase were also present in the FLAG-TPR fusions and absent in the control J257, however the results were not reproducible in the second dataset. It was previously observed that the FLAG affinity tag was incompletely cleaved from the N-terminal TPR chaperone fusion protein in strain J256 (see Chapter 3), which could prevent the detection of some interacting proteins, especially low-abundance proteins. Therefore, proteins identified in J253 but not in J256 or J257 were also considered. A lipoprotein and D-alanyl-D-alanine endopeptidase were identified among the affinity-purified proteins from strain J253 in both data sets. In addition, an ABC transporter, a multidrug transporter, the Tol-Pal system protein TolB, and a membrane protein encoded by AFK24_17180 were exclusively present among the proteins from J253 but only in the one of the data sets.

Discussion

To further understand the role of the T3SS in PGPR *P. syringae* GR12-2, this study attempted to identify proteins that interact with a predicted T3SS chaperone using affinity purification and MS. From the proteins identified using this method, those of the greatest interest are a lipoprotein encoded by AFK24_02690 and a D-alanyl-D-alanine endopeptidase encoded by AFK24_23620. Proteins found exclusively in J253 with total spectrum counts above five but in only one of the datasets, such as an ABC transporter encoded by AFK24_03575 and a multidrug transporter encoded by AFK24_17515, are also of interest and are considered due to the semi-stochastic nature of MS, where low-

Table 4.2. Proteins captured by affinity purification with N- and C-terminal TPR chaperone-FLAG fusion proteins expressed in *P. syringae* J253 and J256, respectively. As a control, proteins were similarly captured in lysates from *P. syringae* J257 which does not express a FLAG-tagged TPR chaperone. The proteins were identified in replicate cultures (sets 1 and 2) by LC/MS/MS.

Identified Protein	Molecular Weight	Accession Number	Gene*	Data Set	Total Spectrum Counts		
					J253	J256	J257
TPR	28 kDa	A0A1C7Z188	20305	Set 1	36	39	0
				Set 2	35	49	0
Lipoprotein	51 kDa	A0A1C7ZDH0	02690	Set 1	21	0	0
				Set 2	6	0	0
D-alanyl-D-alanine endopeptidase	34 kDa	A0A1C7YZC4	23620	Set 1	6	0	0
				Set 2	5	0	0
ABC transporter substrate-binding protein	37 kDa	A0A1C7Z8I9	03575	Set 1	7	0	0
				Set 2	-	-	-
Multidrug transporter	53 kDa	A0A1C7Z379	17515	Set 1	5	0	0
				Set 2	-	-	-
Tol-Pal system protein, TolB	48 kDa	A0A085UPE8	19935	Set 1	9	0	0
				Set 2	-	-	-
Membrane protein	35 kDa	A0A1C7Z4U9	17180	Set 1	6	0	0
				Set 2	-	-	-
Pyridine nucleotide-disulfide oxidoreductase	52 kDa	A0A1C7YW16	27400	Set 1	-	-	-
				Set 2	5	1	0
4-hydroxy-tetrahydrodipicolinate synthase	31 kDa	A0A085UPG0	20000	Set 1	-	-	-
				Set 2	5	1	0

*AFK24 removed from gene locus tag

abundance proteins can go undetected, even in replicates (Barkovits *et al.,* 2020; Tabb *et al.,* 2010).

D-alanyl-D-alanine endopeptidase (D-ala-D-ala endopeptidase) was captured by affinity purification from J253 cultures in both data sets. This enzyme functions in cell wall synthesis, specifically in peptidoglycan (PG) expansion by cleaving the peptide side chains that crosslink the glycan strands, thereby allowing for the insertion of additional PG subunits (Ghosh *et al.,* 2008; Singh *et al.,* 2015). D-ala-D-ala endopeptidases are members of the penicillin-binding protein (PBP) family, named due to their ability to bind β-lactam antibiotics (Ghosh *et al.,* 2008). Many PBPs function as synthases in cell wall synthesis and remodelling in gram-negative bacteria (Greene *et al.,* 2018). Several proteins involved in cell wall synthesis were also identified by MS among the proteins secreted by wild-type *P. syringae* GR12-2 but not by one of the T3SS deletion mutants J246 or J247 (see Chapter 2). These include two D-ala-D-ala carboxypeptidases (encoded by AFK24_13675 and AFK24_15435, respectively) which cleave C-terminal peptide bonds in PG side chains and function with endopeptidases to remodel the cell wall (Ghosh *et al.,* 2008), and LpoB (encoded by AFK24_02700), which is required to activate a major PG synthase with dual roles in side chain polymerization and peptide crosslinking (Egan *et al.,* 2014; Greene *et al.,* 2018). The gene encoding LpoB is adjacent to that of the lipoprotein of interest (encoded by AFK24_02690) in the *P. syringae* GR12-2 genome, separated by one gene encoding a putative lipoprotein (Lewis *et al.,* 2017; Mistry *et al.,* 2021); all three genes are encoded on the same DNA strand, possibly in an operon. While the function of the lipoprotein is unknown, the clustering of the genes encoding the lipoprotein and LpoB may suggest that they function in the same pathway for cell wall modification.

T3SSs span both membranes of gram-negative bacteria and require remodelling of the PG layer during assembly (Burkinshaw *et al.*, 2015; Portaliou *et al.*, 2016). Genomic loci encoding T3SSs in enteropathogenic *E. coli* (EPEC) (Burkinshaw *et al.*, 2015) and *P. syringae* pv. tomato DC3000 (Oh *et al.*, 2007) contain genes encoding PG-lytic enzymes that cleave glycosidic linkages, creating space in the PG (Scheurwater *et al.*, 2008). The activity of these PG-lytic enzymes must be tightly regulated. In EPEC, they interact with the T3SS inner rod, proposed as a form of spatial regulation (Burkinshaw *et al.*, 2015). Another method of regulation could be achieved through PG-lytic enzyme interaction with chaperones. Binding to a chaperone is a mechanism commonly employed by cells to control protein interactions, prevent premature activity of an enzyme, and determine the hierarchy of protein export, including by the T3SS (Alfano & Collmer, 2004; Page & Parsot, 2002; Portaliou *et al.*, 2016). The TPR-containing protein may possibly act as a chaperone for lytic enzymes that function in PG modification to facilitate assembly of the type III secretion apparatus in the cell envelope. If the lipoprotein clustered with LpoB also functions in PG modification, it could also form a complex with T3SS chaperones. This is consistent with the function of TPR-containing chaperones during the early or middle phases of the T3SS (Izoré *et al.*, 2011; Portaliou *et al.*, 2016).

The ABC transporter of interest contains the TroA-like domain (Marchler-Bauer *et al.*, 2016). It has the conserved function of substrate binding for the ABC transport of metal ions and ferric siderophores (Hantke, 2001). The detected interaction between the predicted TPR chaperone and a protein with the conserved binding site for siderophores or metal ions may suggest a role for the T3SS in resource acquisition; uptake of iron is a mechanism by which plant growth-promoting bacteria enhance plant growth (Glick, 2012; Vejan *et al.,* 2016).

The protein of interest identified as a multidrug transporter is an outer membrane lipoprotein that belongs to the NodT family (Marchler-Bauer *et al.*, 2016). NodT family proteins are efflux transporters and can work with ABC, Resistance-Nodulation-Division, and other transporters for the secretion of metal cations, proteins, and lipo-oligosaccharides (Paulsen *et al.,* 1997). A notable function of NodT proteins is their secretion of nodulation factors in Rhizobia species that activate the formation of nitrogen-fixing nodules (Fernández-López *et al.*, 1996; Okazaki *et al.*, 2013; Rivilla *et al.*, 1995). NodT proteins are also a part of the same family of outer membrane transport proteins found in *Pseudomonas species*, such as AprF in *P. aeruginosa* (Rivilla *et al.,* 1995). While the function of the Rhc T3SSs is not fully elucidated, expression of the T3SS is co-regulated with nodulation factor production in Rhizobia (Krause *et al.,* 2002; Wassem *et al.*, 2008). Interestingly, host nodulation signalling has been shown to be activated by Rhc T3SS in the absence of Nod factors in *Bradyrhizobium elkanii* (Okazaki *et al.,* 2013).

The number of proteins identified by affinity purification as interacting with the predicted TPR-containing chaperone was quite small. This may be in part due to the limitations of the methods used in this study. The detection of interacting proteins using affinity purification required that their affinity for the TPR chaperone was sufficient to maintain the interaction during the purification process. Protein interactions with the chaperone that were transient or weak may be precluded from detection by affinity purification. As previously mentioned, another limiting factor may be that low abundance proteins are often not detected in MS analysis due to its semi-stochastic nature (Barkovits *et al.*, 2020; Tabb *et al.*, 2010). Repeating the affinity purification and MS analysis with a larger volume of culture would give a more accurate picture of the protein interactions.

The identity of proteins that interact with the TPR chaperone suggests a heretofore undiscovered role for the predicted chaperone in cell wall remodelling in bacteria. Future work is required to confirm this function and its relationship with the T3SS possibly using TPR chaperone-deficient mutants.

Chapter 5: Applications of PGPR with T3SSs in Agriculture

This study aimed to identify proteins secreted by the T3SS to further understand the secretion system's role in the PGPR *P. syringae* GR12-2. Candidate effectors were identified by MS analysis of proteins secreted by the wild-type but not T3SS mutant strains, in particular a predicted TPR chaperone encoded in the T3SS locus and several alginate biosynthesis proteins. Although the TPR proteins and alginate biosynthesis protein AlgK were confirmed to be secreted in a subsequent biochemical assay, their secretion was not dependent on the T3SS. The predicted TPR chaperone interacts with several proteins involved in cell wall remodeling and may function in assembly of the T3SS in the cell envelope but not be secreted by it. The potential role of T3SS proteins in cell wall modification is supported by the T3SS-dependent secretion of several proteins involved in this process.

The small number of TPR chaperone-interacting proteins identified in this study is partly due to stringent thresholds for considering proteins of interest. Additional proteins can be identified when the MS datasets of affinity purified proteins are analyzed at lower thresholds. For example, when the minimum number of peptides required for protein identification is lowered to four, the Tol-Pal system protein Pal was affinity purified exclusively from J253 in one replicate MS dataset; and was affinity purified from both FLAG-tagged TPR expressing strains and the control strain, with a lower spectrum count compared to the TPR strains, in the second the dataset. When the criteria allows for proteins of interest to have low spectrum counts in the J257 control strain compared to the spectrum counts in the FLAG-tagged TPR expressing strains, BamB and BamD can be identified in one replicates MS dataset. BamA was also affinity purified from J253 and J256 in both datasets, and in J257 with a lower spectrum count in one dataset. The BAM proteins identified above are essential components of the β-barrel assembly machinery (BAM) complex (Knowles *et al.*, 2009). The inclusion of proteins with spectrum counts in the control strain lowers the confidence that the protein was isolated solely due to its interaction with the FLAG-tagged TPR fusion proteins, but may still yield interesting results.

The Tol-Pal system is known to function in outer membrane constriction during cell division (Yakhnina & Bernhardt, 2020) but also functions in virulence, survival (Hirakawa *et al.*, 2022), and transmembrane transport (Duan *et al.*, 2000). TolB (Table 4.2), interacts with outer membrane proteins such as outer membrane porins, Pal, and OmpA proteins (Clavel *et al.*, 1998), several of which were identified in the MS results as extracellular proteins (see Chapter 2). The BAM complex folds and inserts proteins into the outer membrane (Knowles *et al.*, 2009; Wang, X *et al.*, 2021). Secretion of BAM complex protein BamE was identified as T3SS-dependent by MS (see Chapter 2). In addition to the cell wall modification proteins, the T3SS may also require proteins such as TolB, Pal, and BAM for assembly in the cell envelope. These proteins may interact with early-stage chaperones, such as the predicted TPR-chaperone.

Identifying and confirming the proteins and mechanisms required for the function of the T3SS in *P. syringae* GR12-2 helps build the understanding of the secretion systems' role in the PGPR. Most of what is understood about the function of this system is from the *hrp-hrc1* and *hrp-hrc2* systems found in plant pathogenic bacteria. The pathogenic systems primarily function in secreting effectors for virulence and suppressing or evading the host's immune response (Alfano & Collmer, 2004). The little that is known about T3SSs in PGPR suggests an expanded role in biocontrol capabilities (Biessy *et al.,* 2019) and activation of nodulation signalling (Okazaki *et al.*, 2013) in addition to suppression of host defense responses (Jiménez-Guerrero *et al.,* 2022; Tampakaki, 2014).

Understanding the T3SS's role will contribute to the exploitation of PGPR in agricultural applications. The interest in and use of more environmentally friendly alternatives to chemical fertilizers and pesticides is growing, with biofertilizers such as application of PGPR to increase crop yield being of particular interest (Daniel *et al.,* 2022; Khalid *et al.*, 2009). Identifying suitable rhizobacteria for biofertilization requires an understanding of the mechanisms by which they interact with the host plants, how they directly or indirectly benefit the plant, and their effect on the rhizosphere (Khalid *et al.*, 2009; Vessey, 2003).

Strains of PGPR with T3SSs have already shown evidence of plant-growth promotion for agricultural applications. The strain *P. syringae* pv. *syringae* 260-02 (*P. syringae* 260-02), a PGPR, has shown evidence of biocontrol capabilities against phytopathogen *P. syringae* pv. tomato DC3000 on tomato and pepper plants *in vitro* (Passera *et al.,* 2019). The function of the T3SS in *P. syringae* 260-02 has not yet been fully elucidated, and may potentially function in some mechanism of plant growth-promotion. *Pseudomonas* strains such as *P. putida* UW4 (Cheng *et al.,* 2007; Duan *et al.,* 2013) and *Pseudomonas fluorescens* PCL1751 (Cho *et al.,* 2015; Egamberdieva *et al.,* 2010) with non-Rhc T3SS have displayed direct plant growth promotion, and *P.*

fluorescens BBc6R8 (Cusano *et al.*, 2010) and *Pseudomonas sp*. LBUM920 (Biessy *et al.*, 2019) strains with an Rhc T3SS display biocontrol capabilities (Zboralski *et al.*, 2022). While a direct role in plant growth-promotion by the T3SS has not been confirmed for these strains, the known ability of the secretion system to influence plant-bacteria interactions suggests a potential T3SS function in benefitting plant growth. The ability of the T3SS to directly secrete proteins into a host plant could also be utilized through genetic engineering to secrete proteins, heterologous or otherwise, that are beneficial to host plants, such as those involved in decreasing plant stress or biocontrol against pathogens. Identifying the mechanism of plant growth promotion, and the T3SS's potential role in the beneficial effects, could show that *P. syringae* GR12-2 could also be used for agricultural purposes.

This study aimed to further understand the function of the T3SS in *P. syringae* GR12-2, a PGPR, by identifying secreted effectors. While no identified proteins were confirmed to be secreted in a T3SS-dependent manner, this study reports potential secreted effectors and proteins that interact with a predicted T3SS chaperone for further investigation and confirmation. These potential effectors and their functions will further our understanding of T3SSs in PGPR strains like *P. syringae* GR12-2 for potential future use in agricultural advancement.

Bibliography

Abrusci, P., Vergara-Irigaray, M., Johnson, S., Beeby, M. D., Hendrixson, D. R., Roversi, P., Friede, M. E., Deane, J. E., Jensen, G. J., Tang, C. M., & Lea, S. M. (2012). Architecture of the Major Component of the Type III Secretion System Export Apparatus. *Nature Structural & Molecular Biology*, *20*(1), 99–104. https://doi.org/10.1038/nsmb.2452

Ahemad, M., & Kibret, M. (2014). Mechanisms and Applications of Plant Growth Promoting Rhizobacteria: Current Perspective. *Journal of King Saud University - Science*, *26*(1), 1–20. https://doi.org/10.1016/j.jksus.2013.05.001

Akeda, Y., & Galán, J. E. (2005). Chaperone Release and Unfolding of Substrates in Type III Secretion. *Nature*, *437*(7060), 911–915. https://doi.org/10.1038/nature03992

Alfano, J. R., & Collmer, A. (2004). Type III Secretion System Effector Proteins: Double Agents in Bacterial Disease and Plant Defense. *Annual Review of Phytopathology*, *42*(1), 385–414. https://doi.org/10.1146/annurev.phyto.42.040103.110731

Baldwin, M. A. (2004). Protein Identification by Mass Spectrometry: Issues to be Considered. *Molecular & Cellular Proteomics*, *3*(1), 1–9.

Bao, Z., Wei, H.-L., Ma, X., & Swingle, B. (2020). *Pseudomonas syringae* AlgU Downregulates Flagellin Gene Expression, Helping Evade Plant Immunity. *Journal of Bacteriology*, *202*(4). https://doi.org/10.1128/jb.00418-19

Barkovits, K., Pacharra, S., Pfeiffer, K., Steinbach, S., Eisenacher, M., Marcus, K., & Uszkoreit, J. (2020). Reproducibility, Specificity and Accuracy of Relative Quantification Using Spectral Library-Based Data-Independent Acquisition. *Molecular & Cellular Proteomics*, *19*(1), 181–197. https://doi.org/10.1074/mcp.ra119.001714

Best, E. A., & Knauf, V. C. (1993). Organization and Nucleotide Sequences of the Genes Encoding the Biotin Carboxyl Carrier Protein and Biotin Carboxylase Protein of *Pseudomonas aeruginosa* Acetyl Coenzyme A Carboxylase. *Journal of Bacteriology*, *175*(21), 6881–6889. https://doi.org/10.1128/jb.175.21.6881-6889.1993

Biessy, A., Novinscak, A., Blom, J., Léger, G., Thomashow, L. S., Cazorla, F. M., Josic, D., & Filion, M. (2019). Diversity of Phytobeneficial Traits Revealed by Whole-Genome Analysis of Worldwide-Isolated Phenazine-Producing *Pseudomonas* spp.. *Environmental Microbiology*, *21*(1), 437-455. https://doi.org/10.1111/1462-2920.14476

Blakney, A. J. C., & Patten, C. L. (2011). A Plant Growth-promoting Pseudomonad is Closely Related to the *Pseudomonas syringae* Complex of Plant Pathogens. *FEMS Microbiology Ecology*, *77*(3), 546–557. https://doi.org/10.1111/j.1574-6941.2011.01136.x

Bouveret, E., Bénédetti, H., Rigal, A., Loret, E., & Lazdunski, C. (1999). In Vitro Characterization of Peptidoglycan-Associated Lipoprotein (PAL)–Peptidoglycan and PAL–TolB Interactions. *Journal of Bacteriology*, *181*(20), 6306–6311. https://doi.org/10.1128/jb.181.20.6306-6311.1999

Boyd, A., & Chakrabarty, A. M. (1995). *Pseudomonas aeruginosa* Biofilms: Role of the Alginate Exopolysaccharide. *Journal of Industrial Microbiology*, *15*(3), 162–168. https://doi.org/10.1007/bf01569821

Bradford, M. M. (1976). A Rapid and Sensitive Method for the Quantitation of Microgram Quantities of Protein Utilizing the Principle of Protein-Dye Binding. *Analytical Biochemistry*, *72*(1–2), 248–254. https://doi.org/10.1016/0003-2697(76)90527-3

Branon, T. C., Bosch, J. A., Sanchez, A. D., Udeshi, N. D., Svinkina, T., Carr, S. A., Feldman, J. L., Perrimon, N., & Ting, A. Y. (2018). Efficient Proximity Labeling in Living Cells and Organisms with TurboID. *Nature Biotechnology*, *36*(9), 880–887. https://doi.org/10.1038/nbt.4201

Brizzard, B., & Chubet, R. (1997). Epitope tagging of recombinant proteins. *Current Protocols in Neuroscience*, *00*(1), 5.8.1-5.8.10. https://doi.org/10.1002/0471142301.ns0508s00

Bröms, J. E., Edqvist, P. J., Forsberg, Ã., & Francis, M. S. (2006). Tetratricopeptide Repeats are Essential for PcrH Chaperone Function in *Pseudomonas aeruginosa* Type III Secretion. *FEMS Microbiology Letters*, *256*(1), 57–66. https://doi.org/10.1111/j.1574-6968.2005.00099.x

Brzezinska, M., Benveniste, R., Davies, J., Daniels, P. J., & Weinstein, J. (1972). Gentamicin Resistance in Strains of *Pseudomonas aeruginosa* Mediated by Enzymic N-Acetylation of the Deoxystreptamine Moiety. *Biochemistry*, *11*(5), 761–766. https://doi.org/10.1021/bi00755a013

Burkinshaw, B. J., Deng, W., Lameignère, E., Wasney, G. A., Zhu, H., Worrall, L. J., Finlay, B. B., & Strynadka, N. C. J. (2015). Structural Analysis of a Specialized Type III Secretion System Peptidoglycan-Cleaving Enzyme. *Journal of Biological Chemistry*, *290*(16), 10406–10417. https://doi.org/10.1074/jbc.m115.639013

Busciall, P., Chandrasekar, B., Sanguankiattichai, N., Kourelis, J., Kaschani, F., Thomas, E., Morimoto, K., Kaiser, M., Preston, G., Ichinose, Y., & Van Der Hoorn, R.

(2019). Glycosidase and Glycan Polymorphism Control Hydrolytic Release of Immunogenic Flagellin Peptides. *Science, 364*(6436).

Chen, L., Ai, X., Portaliou, A. G., Minetti, C. A. S. A., Remeta, D. P., Economou, A., & Kalodimos, C. G. (2013). Substrate-Activated Conformational Switch on Chaperones Encodes a Targeting Signal in Type III Secretion. *Cell Reports, 3*(5), 1754. https://doi.org/10.1016/j.celrep.2013.05.018

Cheng, Z., Park, E., & Glick, B. R. (2007). 1-Aminocyclopropane-1-Carboxylate Deaminase from *Pseudomonas putida* UW4 Facilitates the Growth of Canola in the Presence of Salt. *Canadian Journal of Microbiology, 53*(7), 912–918. https://doi.org/10.1139/w07-050

Chevalier, S., Bouffartigues, E., Bodilis, J., Maillot, O., Lesouhaitier, O., Feuilloley, M. G., Orange, N., Dufour, A., & Cornelis, P. (2017). Structure, Function and Regulation of *Pseudomonas aeruginosa* Porins. *FEMS Microbiology Reviews, 41*(5), 698–722. https://doi.org/10.1093/femsre/fux020

Chitnis, C. E., & Ohman, D. E. (1993). Genetic Analysis of the Alginate Biosynthetic Gene Cluster of *Pseudomonas aeruginosa* Shows Evidence of an Operonic Structure. *Molecular Microbiology*, *8*(3), 583–590. https://doi.org/10.1111/j.1365-2958.1993.tb01602.x

Cho, S.-T., Chang, H.-H., Egamberdieva, D., Kamilova, F., Lugtenberg, B., & Kuo, C.-H. (2015). Genome Analysis of *Pseudomonas fluorescens* PCL1751: A Rhizobacterium that Controls Root Diseases and Alleviates Salt Stress for Its Plant Host. *PLOS ONE, 10*(10). https://doi.org/10.1371/journal.pone.0140231

Choi-Rhee, E., Schulman, H., & Cronan, J. E. (2008). Promiscuous Protein Biotinylation by *Escherichia coli* Biotin Protein Ligase. *Protein Science*, *13*(11), 3043–3050. https://doi.org/10.1110/ps.04911804

Cerveny, L., Straskova, A., Dankova, V., Hartlova, A., Ceckova, M., Staud, F., & Stulik, J. (2013). Tetratricopeptide Repeat Motifs in the World of Bacterial Pathogens: Role in Virulence Mechanisms. *Infection and Immunity, 81*(3), 629–635. https://doi.org/10.1128/iai.01035-12

Clavel, T., Germon, P., Vianney, A., Portalier, R., & Lazzaroni, J. C. (1998). TolB Protein of *Escherichia coli* K-12 Interacts with the Outer Membrane Peptidoglycan-Associated Proteins Pal, Lpp and OmpA. *Molecular Microbiology*, *29*(1), 359–367. https://doi.org/10.1046/j.1365-2958.1998.00945.x

Cook, J. (2016). Expression of a Type III Secretion System in a Plant Growth-Promoting Bacteria. (*Unpublished Thesis*). UNB.

Cook, T. B., Rand, J. M., Nurani, W., Courtney, D. K., Liu, S. A., & Pfleger, B. F. (2018). Genetic Tools for Reliable Gene Expression and Recombineering in *Pseudomonas putida*. *Journal of Industrial Microbiology and Biotechnology*, *45*(7), 517–527. https://doi.org/10.1007/s10295-017-2001-5

Cusano, A. M., Burlinson, P., Deveau, A., Vion, P., Uroz, S., Preston, G. M., & Frey-Klett, P. (2010). *Pseudomonas fluorescens* BBc6R8 Type III Secretion Mutants No Longer Promote Ectomycorrhizal Symbiosis. *Environmental Microbiology Reports*, *3*(2), 203–210. https://doi.org/10.1111/j.1758-2229.2010.00209.x

D'Andrea, L. (2003). TPR Proteins: The Versatile Helix. *Trends in Biochemical Sciences*, *28*(12), 655–662. https://doi.org/10.1016/j.tibs.2003.10.007

Daniel, A. I., Fadaka, A. O., Gokul, A., Bakare, O. O., Aina, O., Fisher, S., Burt, A. F., Mavumengwana, V., Keyster, M., & Klein, A. (2022). Biofertilizer: The Future of Food Security and Food Safety. *Microorganisms*, *10*(6), 1220. https://doi.org/10.3390/microorganisms10061220

Deng, W., Marshall, N. C., Rowland, J. L., McCoy, J. M., Worrall, L. J., Santos, A. S., Strynadka, N. C., & Finlay, B. B. (2017). Assembly, Structure, Function and Regulation of Type III Secretion Systems. *Nature Reviews Microbiology*, *15*(6), 323–337. https://doi.org/10.1038/nrmicro.2017.20

Dixon, A. S., Schwinn, M. K., Hall, M. P., Zimmerman, K., Otto, P., Lubben, T. H., Butler, B. L., Binkowski, B. F., Machleidt, T., Kirkland, T. A., Wood, M. G., Eggers, C. T., Encell, L. P., & Wood, K. V. (2015). NanoLuc Complementation Reporter Optimized for Accurate Measurement of Protein Interactions in Cells. *ACS Chemical Biology*, *11*(2), 400–408. https://doi.org/10.1021/acschembio.5b00753

Dorfer, V., Pichler, P., Stranzl, T., Stadlmann, J., Taus, T., Winkler, S., & Mechtler, K. (2014). MS Amanda, a Universal Identification Algorithm Optimized for High Accuracy Tandem Mass Spectra. *Journal of Proteome Research*, *13*(8), 3679–3684. https://doi.org/10.1021/pr500202e

Duan, J., Jiang, W., Cheng, Z., Heikkila, J. J., & Glick, B. R. (2013). The Complete Genome Sequence of the Plant Growth-Promoting Bacterium *Pseudomonas* sp. UW4. *PLoS ONE, 8*(3). https://doi.org/10.1371/journal.pone.0058640

Duan, K., Lafontaine, E. R., Majumdar, S., & Sokol, P. A. (2000). RegA, Iron, and Growth Phase Regulate Expression of the *Pseudomonas aeruginosa tol-oprL* Gene Cluster. *Journal of Bacteriology*, *182*(8), 2077–2087. https://doi.org/10.1128/jb.182.8.2077-2087.2000

Edqvist, P. J., Broms, J. E., Betts, H. J., Forsberg, A., Pallen, M. J., & Francis, M. S. (2006). Tetratricopeptide Repeats in the Type III Secretion Chaperone, LcrH: Their Role in Substrate Binding and Secretion. *Molecular Microbiology*, *59*(1), 31–44. https://doi.org/10.1111/j.1365-2958.2005.04923.x

Egamberdieva, D., Kucharova, Z., Davranov, K., Berg, G., Makarova, N., Azarova, T., Chebotar, V., Tikhonovich, I., Kamilova, F., Validov, S. Z., & Lugtenberg, B. (2010). Bacteria Able to Control Foot and Root Rot and to Promote Growth of Cucumber in Salinated Soils. *Biology and Fertility of Soils*, *47*(2), 197–205. https://doi.org/10.1007/s00374-010-0523-3

Egan, A. J., Jean, N. L., Koumoutsi, A., Bougault, C. M., Biboy, J., Sassine, J., Solovyova, A. S., Breukink, E., Typas, A., Vollmer, W., & Simorre, J.-P. (2014). Outer-Membrane Lipoprotein LpoB Spans the Periplasm to Stimulate the Peptidoglycan Synthase PBP1B. *Proceedings of the National Academy of Sciences*, *111*(22), 8197–8202. https://doi.org/10.1073/pnas.1400376111

Eng, J. K., McCormack, A. L., & Yates, J. R. (1994). An Approach to Correlate Tandem Mass Spectral Data of Peptides with Amino Acid Sequences in a Protein Database. *Journal of the American Society for Mass Spectrometry*, *5*(11), 976–989. https://doi.org/10.1016/1044-0305(94)80016-2

Fakhr, M. K., Peñaloza-Vázquez, A., Chakrabarty, A. M., & Bender, C. L. (1999). Regulation of Alginate Biosynthesis in *Pseudomonas syringae* pv. syringae. *Journal of Bacteriology*, *181*(11), 3478–3485. https://doi.org/10.1128/jb.181.11.3478-3485.1999

Fall, R. R., Alberts, A. W., & Vagelos, P. R. (1975). Analysis of Bacterial Biotin-Proteins. *Biochimica et Biophysica Acta (BBA) - Protein Structure*, *379*(2), 496–503. https://doi.org/10.1016/0005-2795(75)90156-7

Feldman, M. F., & Cornelis, G. R. (2003). The Multitalented Type III Chaperones: All You Can Do with 15 kDa. *FEMS Microbiology Letters*, *219*(2), 151–158. https://doi.org/10.1016/s0378-1097(03)00042-9

Fernández-López, M., D'Haeze, W., Mergaert, P., Verplancke, C., Prome, J.-C., Montagu, M., & Holsters, M. (1996). Role of *nodl* and *nodJ* in Lipo-chitooligosaccharide Secretion in *Azorhizobium caulinodans* and *Escherichia coli*. *Molecular Microbiology*, *20*(5), 993–1000. https://doi.org/10.1111/j.1365-2958.1996.tb02540.x

Franklin, M. J., & Ohman, D. E. (1993). Identification of AlgF in the Alginate Biosynthetic Gene Cluster of *Pseudomonas aeruginosa* Which is Required for Alginate Acetylation. *Journal of Bacteriology*, *175*(16), 5057–5065. https://doi.org/10.1128/jb.175.16.5057-5065.1993

Freudl, R., Klose, M., & Henning, U. (1990). Export and Sorting of the *Escherichia coli* Outer Membrane Protein OmpA. *Journal of Bioenergetics and Biomembranes*, *22*(3), 441–449. https://doi.org/10.1007/bf00763176

Gazi, A. D., Sarris, P. F., Fadouloglou, V. E., Charova, S. N., Mathioudakis, N., Panopoulos, N. J., & Kokkinidis, M. (2012). Phylogenetic Analysis of a Gene Cluster Encoding an Additional, Rhizobial-Like Type III Secretion System that is Narrowly Distributed Among *Pseudomonas syringae* Strains. *BMC Microbiology*, *12*(1). https://doi.org/10.1186/1471-2180-12-188

Ghosh, A. S., Chowdhury, C., & Nelson, D. E. (2008). Physiological Functions of D-Alanine Carboxypeptidases in *Escherichia coli*. *Trends in Microbiology*, *16*(7), 309–317. https://doi.org/10.1016/j.tim.2008.04.006

Glick, B. R. (2012). Plant Growth-Promoting Bacteria: Mechanisms and Applications. *Scientifica*, 2012, 1–15. https://doi.org/10.6064/2012/963401

Glish, G. L., & Vachet, R. W. (2003). The Basics of Mass Spectrometry in the Twenty-First Century. *Nature Reviews Drug Discovery*, *2*(2), 140–150. https://doi.org/10.1038/nrd1011

Govan, J. R., Fyfe, J. A., & Jarman, T. R. (1981). Isolation of Alginate-Producing Mutants of *Pseudomonas fluorescens*, *Pseudomonas putida* and *Pseudomonas mendocina*. *Microbiology*, *125*(1), 217–220. https://doi.org/10.1099/00221287-125-1-217

Greene, N. G., Fumeaux, C., & Bernhardt, T. G. (2018). Conserved Mechanism of Cell-Wall Synthase Regulation Revealed by the Identification of a New PBP Activator in *Pseudomonas aeruginosa*. *Proceedings of the National Academy of Sciences*, *115*(12), 3150–3155. https://doi.org/10.1073/pnas.1717925115

Guzman, L. M., Belin, D., Carson, M. J., & Beckwith, J. (1995). Tight Regulation, Modulation, and High-Level Expression by Vectors Containing the Arabinose PBAD Promoter. *Journal of Bacteriology*, *177*(14), 4121–4130. https://doi.org/10.1128/jb.177.14.4121-4130.1995

Hahn, S., Dunn, T., & Schleif, R. (1984). Upstream Repression and CRP Stimulation of the *Escherichia coli* L-Arabinose Operon. *Journal of Molecular Biology*, *180*(1), 61–72. https://doi.org/10.1016/0022-2836(84)90430-3

Hall, J. A., Peirson, D., Ghosh, S., & Glick, B. R. (1996). Root Elongation in Various Agronomic Crops by the Plant Growth Promoting Rhizobacterium *Pseudomonas putida* GR12-2. *Israel J Plant Sci*, *44*(1), 37–42. https://doi.org/10.1080/07929978.1996.10676631

Hall, M. P., Unch, J., Binkowski, B. F., Valley, M. P., Butler, B. L., Wood, M. G., Otto, P., Zimmerman, K., Vidugiris, G., Machleidt, T., Robers, M. B., Benink, H. A., Eggers, C. T., Slater, M. R., Meisenheimer, P. L., Klaubert, D. H., Fan, F., Encell, L. P., & Wood, K. V. (2012). Engineered Luciferase Reporter From a Deep Sea Shrimp Utilizing a Novel Imidazopyrazinone Substrate. *ACS Chemical Biology*, *7*(11), 1848–1857. https://doi.org/10.1021/cb3002478

Hantke, K. (2001). Bacterial Zinc Transporters and Regulators. *Biometals*, *14*, 239–249. https://doi.org/10.1007/978-94-017-3728-9_4

Hay, I. D., Rehman, Z. U., Moradali, M. F., Wang, Y., & Rehm, B. H. (2013). Microbial Alginate Production, Modification and Its Applications. *Microbial Biotechnology*, *6*(6), 637–650. https://doi.org/10.1111/1751-7915.12076

Heredia-Ponce, Z., Gutiérrez-Barranquero, J. A., Purtschert-Montenegro, G., Eberl, L., Cazorla, F. M., & de Vicente, A. (2020). Biological Role of EPS From *Pseudomonas syringae* pv. syringae UMAF0158 Extracellular Matrix, Focusing on a Psl-Like Polysaccharide. *Npj Biofilms and Microbiomes*, *6*(1). https://doi.org/10.1038/s41522-020-00148-6

Hirakawa, H., Suzue, K., & Tomita, H. (2022). Roles of the Tol/Pal System in Bacterial Pathogenesis and Its Application to Antibacterial Therapy. *Vaccines*, *10*(3), 422. https://doi.org/10.3390/vaccines10030422

Hynes, M. (2019). Type III Secretion System of *Pseudomonas syringae* GR12-2: an Investigation into Intercellular Communication. (*Unpublished Thesis*). UNB

Izoré, T., Job, V., & Dessen, A. (2011). Biogenesis, Regulation, and Targeting of the Type III Secretion System. *Structure*, *19*(5), 603–612. https://doi.org/10.1016/j.str.2011.03.015

Jiménez-Guerrero, I., Medina, C., Vinardell, J. M., Ollero, F. J., & López-Baena, F. J. (2022). The Rhizobial Type 3 Secretion System: The Dr. Jekyll and Mr. Hyde in the Rhizobium–Legume Symbiosis. *International Journal of Molecular Sciences*, *23*(19), 11089. https://doi.org/10.3390/ijms231911089

Jong, E. (2018). Identification of Effectors of a Type III Secretion System in a Plant Growth-Promoting Rhizobacterium. (*Unpublished Report*). UNB.

Käll, L., Storey, J. D., & Noble, W. S. (2008). Non-Parametric Estimation of Posterior Error Probabilities Associated with Peptides Identified by Tandem Mass Spectrometry. *Bioinformatics*, *24*(16), 142–148. https://doi.org/10.1093/bioinformatics/btn294

Kaschani, F., Wei, Q., Dingemans, J., van der Hoorn, R. A. L., Cornelis, P., & Kaiser, M. (2016). Capture of Endogenously Biotinylated Proteins from *Pseudomonas aeruginosa* Displays Unexpected Downregulation of LiuD Upon Iron Nutrition. *Bioorganic & Medicinal Chemistry*, *24*(15), 3330–3335. https://doi.org/10.1016/j.bmc.2016.04.051

Katagiri, F., Thilmony, R., & He, S. Y. (2002). The Arabidopsis Thaliana-Pseudomonas Syringae Interaction. *The Arabidopsis Book*, *1*. https://doi.org/10.1199/tab.0039

Keiski, C.-L., Harwich, M., Jain, S., Neculai, A. M., Yip, P., Robinson, H., Whitney, J. C., Riley, L., Burrows, L. L., Ohman, D. E., & Howell, P. L. (2010). Algk is a TPR-Containing Protein and the Periplasmic Component of a Novel Exopolysaccharide Secretin. *Structure*, *18*(2), 265–273. https://doi.org/10.1016/j.str.2009.11.015

Khalid, A., Arshad, M., Shaharoona, B., & Mahmood, T. (2009). Plant Growth Promoting Rhizobacteria and Sustainable Agriculture. *Microbial Strategies for Crop Improvement*, 133–160. https://doi.org/10.1007/978-3-642-01979-1_7

Kim, D. I., Jensen, S. C., Noble, K. A., KC, B., Roux, K. H., Motamedchaboki, K., & Roux, K. J. (2016). An Improved Smaller Biotin Ligase for BioID Proximity Labeling. *Molecular Biology of the Cell*, *27*(8), 1188–1196. https://doi.org/10.1091/mbc.e15-12-0844

Kim, D. I., KC, B., Zhu, W., Motamedchaboki, K., Doye, V., & Roux, K. J. (2014). Probing Nuclear Pore Complex Architecture with Proximity-Dependent Biotinylation. *Proceedings of the National Academy of Sciences*, *111*(24), 2453-2461. https://doi.org/10.1073/pnas.1406459111

Knowles, T. J., Scott-Tucker, A., Overduin, M., & Henderson, I. R. (2009). Membrane Protein Architects: The Role of the BAM Complex in Outer Membrane Protein Assembly. *Nature Reviews Microbiology*, *7*(3), 206–214. https://doi.org/10.1038/nrmicro2069

Konovalova, A., & Silhavy, T. J. (2015). Outer Membrane Lipoprotein Biogenesis: Lol is Not the End. *Philosophical Transactions of the Royal Society B: Biological Sciences*, *370*(1679), 20150030. https://doi.org/10.1098/rstb.2015.0030

Koo, J., Tammam, S., Ku, S.-Y., Sampaleanu, L. M., Burrows, L. L., & Howell, P. L. (2008). PilF is an Outer Membrane Lipoprotein Required for Multimerization and Localization of the *Pseudomonas aeruginosa* Type IV Pilus Secretin. *Journal of Bacteriology*, *190*(21), 6961–6969. https://doi.org/10.1128/jb.00996-08

Krause, A., Doerfel, A., & Göttfert, M. (2002). Mutational and Transcriptional Analysis of the Type III Secretion System of *Bradyrhizobium japonicum*. *Molecular Plant-*

Microbe Interactions, *15*(12), 1228–1235. https://doi.org/10.1094/mpmi.2002.15.12.1228

Krishna, P. S., Woodcock, S. D., Pfeilmeier, S., Bornemann, S., Zipfel, C., & Malone, J. G. (2021). *Pseudomonas syringae* Addresses Distinct Environmental Challenges During Plant Infection Through the Coordinated Deployment of Polysaccharides. *Journal of Experimental Botany*, *73*(7), 2206–2221. https://doi.org/10.1093/jxb/erab550

Lee, S., & Lee, D. K. (2020). What is the Proper Way to Apply the Multiple Comparison Test? *Korean Journal of Anesthesiology*, *73*(6), 572–572. https://doi.org/10.4097/kja.d.18.00242.e1

Lewis, T. E., Sillitoe, I., Dawson, N., Lam, S. D., Clarke, T., Lee, D., Orengo, C., & Lees, J. (2017). Gene3D: Extensive Prediction of Globular Domains in Proteins. *Nucleic Acids Research*, *46*(D1), 435-439. https://doi.org/10.1093/nar/gkx1069

Lifshitz, R., Kloepper, J. W., Kozlowski, M., Simonson, C., Carlson, J., Tipping, E. M., & Zaleska, I. (1987). Growth Promotion of Canola (Rapeseed) Seedlings by a Strain of *Pseudomonas putida* Under Gnotobiotic Conditions. *Canadian Journal of Microbiology*, *33*(5), 390-395. doi:10.1139/m87-068

Lifshitz, R., Kloepper, J. W., Scher, F. M., Tipping, E. M., & Laliberté, M. (1986). Nitrogen-Fixing Pseudomonads Isolated from Roots of Plants Grown in the Canadian High Arctic. *Applied and Environmental Microbiology*, *51*(2), 251-255. doi:10.1128/aem.51.2.251-255.1986

Lugtenberg, B., & Kamilova, F. (2009). Plant-Growth-Promoting Rhizobacteria. *Annual Review of Microbiology*, *63*(1), 541–556. https://doi.org/10.1146/annurev.micro.62.081307.162918

Macho, A. P., & Zipfel, C. (2015). Targeting of Plant Pattern Recognition Receptor-Triggered Immunity by Bacterial Type-III Secretion System Effectors. *Current Opinion in Microbiology*, *23*, 14–22. https://doi.org/10.1016/j.mib.2014.10.009

Marchler-Bauer, A., Bo, Y., Han, L., He, J., Lanczycki, C. J., Lu, S., Chitsaz, F., Derbyshire, M. K., Geer, R. C., Gonzales, N. R., Gwadz, M., Hurwitz, D. I., Lu, F., Marchler, G. H., Song, J. S., Thanki, N., Wang, Z., Yamashita, R. A., Zhang, D., Zheng, C., Geer, L., & Bryant, S. H. (2016). CDD/SPARCLE: Functional Classification of Proteins via Subfamily Domain Architectures. *Nucleic Acids Research*, *45*(D1), 200-203. https://doi.org/10.1093/nar/gkw1129

Markel, E., Stodghill, P., Bao, Z., Myers, C. R., & Swingle, B. (2016). AlgU Controls Expression of Virulence Genes in *Pseudomonas syringae* pv. tomato DC3000. *Journal of Bacteriology*, *198*(17), 2330–2344. https://doi.org/10.1128/jb.00276-16

Maunders, E., & Welch, M. (2017). Matrix Exopolysaccharides; the Sticky Side of Biofilm Formation. *FEMS Microbiology Letters*, *364*(13). https://doi.org/10.1093/femsle/fnx120

Meisner, J., & Goldberg, J. B. (2016). The *Escherichia coli rhaSR-PrhaBAD* Inducible Promoter System Allows Tightly Controlled Gene Expression Over a Wide Range *in Pseudomonas aeruginosa*. *Applied and Environmental Microbiology*, *82*(22), 6715–6727. https://doi.org/10.1128/aem.02041-16

Mistry, J., Chuguransky, S., Williams, L., Qureshi, M., Salazar, G. A., Sonnhammer, E. L. L., Tosatto, S. C., Paladin, L., Raj, S., Richardson, L. J., Finn, R. D., & Bateman, A. (2021). Pfam: The Protein Families Database in 2021. *Nucleic Acids Res*, *49*(D1), 412–419. https://doi.org/doi: 10.1093/nar/gkaa913

Nesvizhskii, A. I., Keller, A., Kolker, E., & Aebersold, R. (2003). A Statistical Model for Identifying Proteins by Tandem Mass Spectrometry. *Analytical Chemistry*, *75*(17), 4646–4658. https://doi.org/10.1021/ac0341261

Ochsner, U. A., Vasil, A. I., Johnson, Z., & Vasil, M. L. (1999). *Pseudomonas aeruginosa fur* Overlaps with a Gene Encoding a Novel Outer Membrane Lipoprotein, OmlA. *Journal of Bacteriology*, *181*(4), 1099–1109. https://doi.org/10.1128/jb.181.4.1099-1109.1999

Oh, H.-S., Kvitko, B. H., Morello, J. E., & Collmer, A. (2007). *Pseudomonas syringae* Lytic Transglycosylases Coregulated with the Type III Secretion System Contribute to the Translocation of Effector Proteins into Plant Cells. *Journal of Bacteriology*, *189*(22), 8277–8289. https://doi.org/10.1128/jb.00998-07

Okazaki, S., Kaneko, T., Sato, S., & Saeki, K. (2013). Hijacking of Leguminous Nodulation Signaling by the Rhizobial Type III Secretion System. *Proceedings of the National Academy of Sciences*, *110*(42), 17131–17136. https://doi.org/10.1073/pnas.1302360110

Page, A.-L., & Parsot, C. (2002). Chaperones of the Type III Secretion Pathway: Jacks of All Trades. *Molecular Microbiology*, *46(*1), 1–11. https://doi.org/10.1046/j.1365-2958.2002.03138.x

Pallen, M. J., Francis, M. S., & Futterer, K. (2003). Tetratricopeptide Repeats in Type III Secretion Chaperones and Regulators. *FEMS Microbiology Letters, 223*(1), 53-60. https://doi.org/10.2210/pdb1oom/pdb

Passera, A., Compant, S., Casati, P., Maturo, M. G., Battelli, G., Quaglino, F., Antonielli, L., Salerno, D., Brasca, M., Toffolatti, S. L., Mantegazza, F., Delledonne, M., & Mitter, B. (2019). Not Just a Pathogen? Description of a Plant-Beneficial

Pseudomonas syringae Strain. *Frontiers in Microbiology*, *10*. https://doi.org/10.3389/fmicb.2019.01409

Patten, C. L., Jeong, H., Blakney, A. J., & Wallace, N. (2016). Draft Genome Sequence of a Diazotrophic, Plant Growth–Promoting Rhizobacterium of the *Pseudomonas syringae* Complex. *Genome Announcements*, *4(*5). https://doi.org/10.1128/genomea.01023-16

Paulsen, I., Park, J., Choi, P., & Saierjr, M. (1997). A Family of Gram-Negative Bacterial Outer Membrane Factors that Function in the Export of Proteins, Carbohydrates, Drugs and Heavy Metals From Gram-Negative Bacteria. *FEMS Microbiology Letters*, *156*(1), 1–8. https://doi.org/10.1016/s0378-1097(97)00379-0

Paulsson, M., Kragh, K. N., Su, Y.-C., Sandblad, L., Singh, B., Bjarnsholt, T., & Riesbeck, K. (2021). Peptidoglycan-Binding Anchor is a *Pseudomonas aeruginosa* OmpA Family Lipoprotein With Importance for Outer Membrane Vesicles, Biofilms, and the Periplasmic Shape. *Frontiers in Microbiology, 12*. https://doi.org/10.3389/fmicb.2021.639582

Peñaloza-Vázquez, A., Kidambi, S. P., Chakrabarty, A. M., & Bender, C. L. (1997). Characterization of the Alginate Biosynthetic Gene Cluster in *Pseudomonas syringae* pv. syringae. *Journal of Bacteriology*, *179*(14), 4464–4472. https://doi.org/10.1128/jb.179.14.4464-4472.1997

Pérez-Torres, I., Zuniga-Munoz, A., & Guarner-Lans, V. (2016). Beneficial Effects of the Amino Acid Glycine. *Mini-Reviews in Medicinal Chemistry*, *17*(1), 15–32. https://doi.org/10.2174/1389557516666160609081602

Perkins, D. N., Pappin, D. J., Creasy, D. M., & Cottrell, J. S. (1999). Probability-Based Protein Identification by Searching Sequence Databases Using Mass Spectrometry Data. *Electrophoresis*, *20*(18), 3551–3567. https://doi.org/10.1002/(sici)1522-2683(19991201)20:18<3551::aid-elps3551>3.0.co;2-2

Portaliou, A. G., Tsolis, K. C., Loos, M. S., Zorzini, V., & Economou, A. (2016). Type III Secretion: Building and Operating a Remarkable Nanomachine. *Trends in Biochemical Sciences*, *41*(2), 175–189. https://doi.org/10.1016/j.tibs.2015.09.005

Pozidis, C., Chalkiadaki, A., Gomez-Serrano, A., Stahlberg, H., Brown, I., Tampakaki, A. P., Lustig, A., Sianidis, G., Politou, A. S., Engel, A., Panopoulos, N. J., Mansfield, J., Pugsley, A. P., Karamanou, S., & Economou, A. (2003). Type III Protein Translocase: HrcN is a Peripheral Membrane ATPase that is Activated by Oligomerization. *Journal of Biological Chemistry, 278*(28), 25816-25824. https://doi.org/10.1074/jbc.M301903200

Promega. (2017). Nano-Glo HiBiT Extracellular Detection System. https://www.promega.ca/-/media/files/resources/protocols/technical-manuals/500/nano-glo-hibit-extracellular-detection-system-technical-manual.pdf?rev=563b05c828674a2cbdef8c5ee6e12086&sc_lang=en Accessed: March 26, 2023.

Qin, W., Cho, K. F., Cavanagh, P. E., & Ting, A. Y. (2021). Deciphering Molecular Interactions by Proximity Labeling. *Nature Methods*, *18*(2), 133–143. https://doi.org/10.1038/s41592-020-01010-5

Qiu, D., Eisinger, V. M., Head, N. E., Pier, G. B., & Yu, H. D. (2008a). ClpXP Proteases Positively Regulate Alginate Overexpression and Mucoid Conversion in *Pseudomonas aeruginosa*. *Microbiology*, *154*(7), 2119–2130. https://doi.org/10.1099/mic.0.2008/017368-0

Qiu, D., Damron, F. H., Mima, T., Schweizer, H. P., & Yu, H. D. (2008b). PBAD-Based Shuttle Vectors for Functional Analysis of Toxic and Highly Regulated Genes in *Pseudomonas* and *Burkholderia* spp. and Other Bacteria. *Applied and Environmental Microbiology*, *74*(23), 7422–7426. https://doi.org/10.1128/aem.01369-08

Quandt, J., & Hynes, M. F. (1993). Versatile Suicide Vectors Which Allow Direct Selection for Gene Replacement in Gram-Negative Bacteria. *Gene*, *127*(1), 15–21. https://doi.org/10.1016/0378-1119(93)90611-6

Remans, K., Vercammen, K., Bodilis, J., & Cornelis, P. (2010). Genome-Wide Analysis and Literature-Based Survey of Lipoproteins in *Pseudomonas aeruginosa*. *Microbiology*, *156*(9), 2597–2607. https://doi.org/10.1099/mic.0.040659-0

Remminghorst, U., & Rehm, B. H. A. (2006). Alg44, a Unique Protein Required for Alginate Biosynthesis in *Pseudomonas aeruginosa*. *FEBS Letters*, *580*(16), 3883–3888. https://doi.org/10.1016/j.febslet.2006.05.077

Resing, K. A., & Ahn, N. G. (2004). Proteomics Strategies for Protein Identification. *FEBS Letters*, *579*(4), 885–889. https://doi.org/10.1016/j.febslet.2004.12.001

Rivilla, R., Sutton, J. M., & Downie, J. A. (1995). *Rhizobium Leguminosarum* Nodt is Related to a Family of Outer-Membrane Transport Proteins that Includes TolC, PrtF, CyaE and AprF. *Gene, 161*(1), 27–31. https://doi.org/10.1016/0378-1119(95)00235-x

Rodriguez, E. L., Poddar, S., Iftekhar, S., Suh, K., Woolfork, A. G., Ovbude, S., Pekarek, A., Walters, M., Lott, S., & Hage, D. S. (2020). Affinity Chromatography: A Review of Trends and Developments Over the Past 50 Years. *Journal of Chromatography B, 1157*, 122332. https://doi.org/10.1016/j.jchromb.2020.122332

Rojo, F. (2010). Carbon Catabolite Repression in *Pseudomonas*: Optimizing Metabolic Versatility and Interactions with the Environment. *FEMS Microbiology Reviews*, *34*(5), 658–684. https://doi.org/10.1111/j.1574-6976.2010.00218.x

Roux, K. J., Kim, D. I., Raida, M., & Burke, B. (2012). A Promiscuous Biotin Ligase Fusion Protein Identifies Proximal and Interacting Proteins in Mammalian Cells. *Journal of Cell Biology*, *196*(6), 801–810. https://doi.org/10.1083/jcb.201112098

Satiaputra, J., Shearwin, K. E., Booker, G. W., & Polyak, S. W. (2016). Mechanisms of Biotin-Regulated Gene Expression in Microbes. *Synthetic and Systems Biotechnology*, *1*(1), 17–24. https://doi.org/10.1016/j.synbio.2016.01.005

Scheurwater, E., Reid, C., & Clarke, A. (2008). Lytic Transglycosylases: Bacterial Space-Making Autolysins. *The International Journal of Biochemistry & Cell Biology*, *40*(4), 586–591. https://doi.org/10.1016/j.biocel.2007.03.018

Schiller, N. L., Monday, S. R., Boyd, C. M., Keen, N. T., & Ohman, D. E. (1993). Characterization of the *Pseudomonas aeruginosa* Alginate Lyase Gene (*algL*): Cloning, Sequencing, and Expression in *Escherichia coli*. *Journal of Bacteriology*, *175*(15), 4780–4789. https://doi.org/10.1128/jb.175.15.4780-4789.1993

Schreiber, K. J., & Desveaux, D. (2011). AlgW Regulates Multiple *Pseudomonas syringae* Virulence Strategies. *Molecular Microbiology*, *80*(2), 364–377. https://doi.org/10.1111/j.1365-2958.2011.07571.x

Searle, B. C. (2010). Scaffold: A Bioinformatic Tool for Validating MS/MS-Based Proteomic Studies. *PROTEOMICS*, *10*(6), 1265–1269. https://doi.org/10.1002/pmic.200900437

Shi, Y., Cao, Q., Sun, J., Hu, X., Su, Z., Xu, Y., Zhang, H., Lan, L., & Feng, Y. (2023). The Opportunistic Pathogen *Pseudomonas aeruginosa* Exploits Bacterial Biotin Synthesis Pathway to Benefit Its Infectivity. *PLOS Pathogens*, *19*(1). https://doi.org/10.1371/journal.ppat.1011110

Singh, S. K., Parveen, S., SaiSree, L., & Reddy, M. (2015). Regulated Proteolysis of a Cross-link–Specific Peptidoglycan Hydrolase Contributes to Bacterial Morphogenesis. *Proceedings of the National Academy of Sciences*, *112*(35), 10956–10961. https://doi.org/10.1073/pnas.1507760112

Smith, S. G. J., Mahon, V., Lambert, M. A., & Fagan, R. P. (2007). A Molecular Swiss Army Knife: OmpA Structure, Function and Expression. *FEMS Microbiology Letters*, *273*(1), 1–11. https://doi.org/10.1111/j.1574-6968.2007.00778.x

Stocek, M. (2018). Identification of Type III Secretion System Effector Proteins and Chaperones of Plant-Growth Promoting Rhizobacterium *Pseudomonas syringae* GR12-2. (*Unpublished Thesis*). UNB.

Tabb, D. L., Vega-Montoto, L., Rudnick, P. A., Variyath, A. M., Ham, A.-J. L., Bunk, D. M., Kilpatrick, L. E., Billheimer, D. D., Blackman, R. K., Cardasis, H. L., Carr, S. A., Clauser, K. R., Jaffe, J. D., Kowalski, K. A., Neubert, T. A., Regnier, F. E., Schilling, B., Tegeler, T. J., Wang, M., Wang, P., Whiteaker, J. R., Zimmerman, L. J., Fisher, S. J., Gibson, B. W., Kinsinger, C. R., Mesri, M., Rodriguez, H., Stein, S. E., Tempst, P., Paulovich, A. G., Liebler, D. C., & Spiegelman, C. (2010). Repeatability and Reproducibility in Proteomic Identifications by Liquid Chromatography−Tandem Mass Spectrometry. *Journal of Proteome Research*, *9*(2), 761–776. https://doi.org/10.1021/pr9006365

Tampakaki, A. P. (2014). Commonalities and Differences of T3SSs in Rhizobia and Plant Pathogenic Bacteria. *Frontiers in Plant Science*, *5,* 1-19. https://doi.org/10.3389/fpls.2014.00114

Thomas, P. D., Ebert, D., Muruganujan, A., Mushayahama, T., Albou, L., & Mi, H. (2021). PANTHER: Making Genome-Scale Phylogenetics Accessible to All. *Protein Science*, *31*(1), 8–22. https://doi.org/10.1002/pro.4218

Thomas, S. N., French, D., Jannetto, P. J., Rappold, B. A., & Clarke, W. A. (2022). Liquid Chromatography–Tandem Mass Spectrometry for Clinical Diagnostics. *Nature Reviews Methods Primers*, *2*(98). https://doi.org/10.1038/s43586-022-00187-7

Varnaitė, R., & MacNeill, S. A. (2016). Meet the Neighbors: Mapping Local Protein Interactomes by Proximity-Dependent Labeling with BioID. *PROTEOMICS*, *16*(19), 2503–2518. https://doi.org/10.1002/pmic.201600123

Vejan, P., Abdullah, R., Khadiran, T., Ismail, S., & Nasrulhaq Boyce, A. (2016). Role of Plant Growth Promoting Rhizobacteria in Agricultural Sustainability—A Review. *Molecules*, *21*(5), 573. https://doi.org/10.3390/molecules21050573

Vessey, J. (2003). Plant Growth Promoting Rhizobacteria as Biofertilizers. *Plant and Soil*, *255*, 571–586. https://doi.org/https://doi.org/10.1023/A:1026037216893

Wang, H., Yang, Z., Swingle, B., & Kvitko, B. H. (2021). AlgU, a Conserved Sigma Factor Regulating Abiotic Stress Tolerance and Promoting Virulence in *Pseudomonas syringae*. *Molecular Plant-Microbe Interactions*, *34*(4), 326–336. https://doi.org/10.1094/mpmi-

Wang, X., Peterson, J. H., & Bernstein, H. D. (2021). Bacterial Outer Membrane Proteins are Targeted to the Bam Complex by Two Parallel Mechanisms. *mBio*, *12*(3). https://doi.org/10.1128/mbio.00597-21

Wassem, R., Kobayashi, H., Kambara, K., Le Quéré, A., Walker, G. C., Broughton, W. J., & Deakin, W. J. (2008). TtsI Regulates Symbiotic Genes in *Rhizobium* Species NGR234 by Binding to *tts* Boxes. *Molecular Microbiology*, *68*(3), 736–748. https://doi.org/10.1111/j.1365-2958.2008.06187.x

Williams McMackin, E. A., Corley, J. M., Karash, S., Marden, J., Wolfgang, M. C., & Yahr, T. L. (2021). Cautionary Notes on the Use of Arabinose- and Rhamnose-Inducible Expression Vectors in *Pseudomonas aeruginosa*. *Journal of Bacteriology*. *203*(16), https://doi.org/10.1128/jb.00224-21

Wilson, M. M., & Bernstein, H. D. (2016). Surface-Exposed Lipoproteins: An Emerging Secretion Phenomenon in Gram-Negative Bacteria. *Trends in Microbiology, 24*(3), 198–208. https://doi.org/10.1016/j.tim.2015.11.006

Winsor, G. L., Griffiths, E. J., Lo, R., Dhillon, B. K., Shay, J. A., & Brinkman, F. S. L. (2015). Enhanced Annotations and Features for Comparing Thousands of *Pseudomonas* Genomes in the Pseudomonas Genome Database. *Nucleic Acids Research*, *44*(D1), 646-653. https://doi.org/10.1093/nar/gkv1227

Wu, W., Badrane, H., Arora, S., Baker, H. V., & Jin, S. (2004). MucA-Mediated Coordination of Type III Secretion and Alginate Synthesis in *Pseudomonas aeruginosa*. *Journal of Bacteriology*, *186*(22), 7575–7585. https://doi.org/10.1128/jb.186.22.7575-7585.2004

Wysocki, V. H., Resing, K. A., Zhang, Q., & Cheng, G. (2005). Mass Spectrometry of Peptides and Proteins. *Methods*, *35*(3), 211–222. https://doi.org/10.1016/j.ymeth.2004.08.013

Xin, X.-F., Kvitko, B., & He, S. Y. (2018). *Pseudomonas syringae:* What it Takes to Be a Pathogen. *Nature Reviews Microbiology*, *16*(5), 316–328. https://doi.org/10.1038/nrmicro.2018.17

Yakhnina, A. A., & Bernhardt, T. G. (2020). The Tol-PAL System is Required for Peptidoglycan-Cleaving Enzymes to Complete Bacterial Cell Division. *Proceedings of the National Academy of Sciences*, *117*(12), 6777–6783. https://doi.org/10.1073/pnas.1919267117

Yu, J., Penaloza-Vazquez, A., Chakrabarty, A. M., & Bender, C. L. (1999). Involvement of the Exopolysaccharide Alginate in the Virulence and Epiphytic Fitness of *Pseudomonas syringae* pv. syringae. *Molecular Microbiology*, *33*(4), 712–720. https://doi.org/10.1046/j.1365-2958.1999.01516.x

Zboralski, A., Biessy, A., & Filion, M. (2022). Bridging the Gap: Type III Secretion Systems in Plant-Beneficial Bacteria. *Microorganisms*, *10*(1), 187. https://doi.org/10.3390/microorganisms10010187

Zhang, Y., Fonslow, B. R., Shan, B., Baek, M.-C., & Yates, J. R. (2013). Protein Analysis by Shotgun/Bottom-Up Proteomics. *Chemical Reviews*, *113*(4), 2343–2394. https://doi.org/10.1021/cr3003533

Zhao, X., Bitsch, S., Kubitz, L., Schmitt, K., Deweid, L., Roehrig, A., Barazzone, E. C., Valerius, O., Kolmar, H., & Béthune, J. (2021). UltraID: A Compact and Efficient Enzyme for Proximity-Dependent Biotinylation in Living Cells. *BioRxiv*. https://doi.org/10.1101/2021.06.16.448656

Zückert, W. R. (2014). Secretion of Bacterial Lipoproteins: Through the Cytoplasmic Membrane, the Periplasm and Beyond. *Biochimica et Biophysica Acta (BBA) - Molecular Cell Research*, *1843*(8), 1509–1516. https://doi.org/10.1016/j.bbamcr.2014.04.022

Appendix

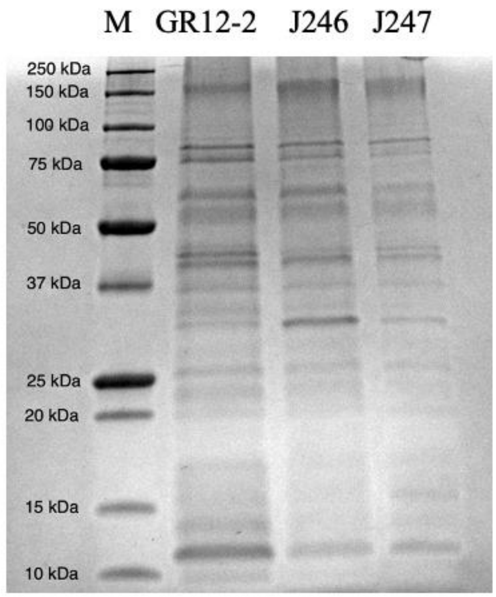

Figure 2.1. Extracellular proteins secreted by wild-type *P. syringae* GR12-2 and T3SS mutants J246 and J247. For each protein sample, three μg of proteins were run on a 4-20% precast-TGX Protein gel at 200V for 30 minutes and stained with Biosafe Coomassie. Unstained Precision Plus Protein Standard (BioRad) was loaded as a marker (M).

Curriculum Vitae

Candidate's full name: Emma Marie Lewis

Universities attended:

University of New Brunswick

September 2016 to May 2020

Bachelor of Science (Biology)